Sillanpää, Sampo

Publication J3/2008

Thermodynamic studies in flow metrology

Sampo Sillanpää

Doctoral Dissertation
Helsinki University of Technology

Thermodynamic studies in flow metrology

J3/2008

Espoo 2009

MIKES Metrology
Espoo 2009

THERMODYNAMIC STUDIES IN FLOW METROLOGY

Doctoral Dissertation

Sampo Sillanpää

Dissertation for the degree of Doctor of Science in Technology to be presented with due permission of the Faculty of Engineering and Architecture for public examination and debate in Auditorium K216 at Helsinki University of Technology (Espoo, Finland) on the 30th of January, 2009, at 12 noon.

ABSTRACT OF DOCTORAL DISSERTATION	MIKES P. O. BOX 9, FI-02151 ESPOO http://www.mikes.fi

Author Sampo Sillanpää

Name of the dissertation

Thermodynamic studies in flow metrology

Manuscript submitted August 6, 2008	Manuscript revised November 19, 2008
Date of the defence January 30, 2009	
☐ Monograph	☒ Article dissertation (summary + original articles)

Faculty	Faculty of Engineering and Architecture
Department	Department of Energy Technology
Field of research	Applied Thermodynamics
Opponent(s)	Professor Riitta Keiski and Dr. Peter Lau
Supervisor	Professor Markku J. Lampinen
Instructor	D.Sc. (Tech) Martti Heinonen

Abstract

Thermodynamic studies in flow metrology were carried out to improve the realization of fluid flow quantities. First, a metrological competence study of the dynamic gravimetric gas mass flow rate measurement standard of MIKES was carried out. Then, a theoretical and experimental study to clarify the varying shear stress on the cylindrical surfaces and its contribution to the combined standard uncertainty of a dynamic gravimetric gas mass flow rate standard was presented. A new mixing method for establishing a traceability link between air velocity standard and national standards of mass and time was developed. The method for compensating the effect of vertical density gradients in a liquid sample to the reading of a hydrometer was developed.

In the dynamic gravimetric gas mass flow rate measurement method, the varying shear stress on the wall of the gas cylinder was studied by time averaging the instantaneous shear stress, calculated from the numerical similarity solution of laminar boundary layer equations. The model was studied experimentally by a balance combined with temperature measurements.

The most commonly used primary standard in air velocity measurements is based on laser anemometry enabling the traceability to the SI base units of length and time. In this study, an alternative method of establishing the traceability link was developed. The method is based on humidification of air in the wind tunnel with the known mass flow rate of water. The air velocity can then be expressed as a function of humidification water mass flow rate enabling the traceability to the SI base units of mass and time. The method was studied in the wind tunnel of MIKES with a Pitot tube.

The non-homogeneous vertical temperature distribution in the liquid sample causes errors in the reading of a hydrometer. In this thesis, a mathematical model for compensating for the effect of temperature gradients has been presented. The model was studied experimentally in the hydrometer calibration system at MIKES. The compensation model improves, for example, the accuracy of conversion between the mass and volume flow rate units.

The methods presented in this thesis can be applied to improve the accuracy of primary standards for small gas flow meters and hydrometers. The mixing method provides a novel and less expensive way to establish the traceability link for air velocity measurements.

Keywords	Flow metrology, thermodynamics, gas mass flow rate, air velocity, liquid density	
ISBN (printed)	978-952-5610-48-2	ISSN (printed) 1235-2704
ISBN (pdf)	978-952-5610-49-9	ISSN (pdf) 1797-9730
Language	English	Number of pages 84 p. + articles 46 p.
Publisher	Centre for Metrology and Accreditation	
Print distribution	Centre for Metrology and Accreditation	

☒ The dissertation can be read at http://lib.tkk.fi/Diss/2009/isbn9789525610499/

VÄITÖSKIRJAN TIIVISTELMÄ	MIKES PL 9, 02151 ESPOO http://www.mikes.fi

Tekijä Sampo Sillanpää

Väitöskirjan nimi

Termodynaamisia tutkimuksia virtausmetrologiasta

Käsikirjoituksen päivämäärä 6.8.2008	Korjatun käsikirjoituksen päivämäärä 19.11.2008
Väitöstilaisuuden ajankohta 30.1.2009	
☐ Monografia	☒ Yhdistelmäväitöskirja (yhteenveto + erillisartikkelit)

Tiedekunta	Insinööritieteiden ja arkkitehtuurin tiedekunta
Laitos	Energiatekniikan laitos
Tutkimusala	Sovellettu termodynamiikka
Vastaväittäjä(t)	Prof. Riitta Keiski ja Dr. Peter Lau
Työn valvoja	Prof. Markku J. Lampinen
Työn ohjaaja	TkT Martti Heinonen

Tiivistelmä

Työssä tutkittiin virtausmetrologian termodynaamisia ilmiöitä virtaussuureiden mittayksiköiden kehittämiseksi. Ensimmäiseksi tutkittiin MIKESin dynaamiseen punnitukseen perustuvan kaasun massavirran mittanormaalin metrologista kompetenssia. Tämän jälkeen selvitettiin ajasta riippuvan luonnollisen konvektiovirtauksen aiheuttamaa leikkausjännitystä sylinterimäisten kappaleiden pinnalla ja leikkausjännityksen vaihtelun aiheuttaman epävarmuuskomponentin suuruutta dynaamiseen punnitukseen perustuvan kaasun massavirran mittanormaalissa. Dynaamista punnitusmenetelmää hyödyntäen kehitettiin ilman virtausnopeudelle mittausmenetelmä, jonka avulla virtausnopeuden mittanormaali pystytään kytkemään massan ja ajan kansallisiin mittanormaaleihin. Lisäksi tutkittiin nestenäytteen pystysuorien lämpötilagradienttien vaikutusta areometrin näyttämään ja kehitettiin matemaattinen malli gradienttien vaikutuksen kompensoimiseksi.

Dynaamisessa punnitusmenetelmässä kaasusäiliön seinämässä esiintyvän luonnollisen konvektiovirtauksen aiheuttamaa vaihtelevaa leikkausjännitystä mallinnettiin aikakeskiarvottamalla laminaarin rajakerroksen virtausyhtälöiden numeerisen similariteettiratkaisun perusteella laskettua leikkausjännitystä. Mallin toimivuutta testattiin kokeellisesti vaa'an ja lämpötilamittauksen avulla.

Yleisimmin ilman virtausnopeusmittauksen jäljitettävyys metrologisissa tuulitunneleissa perustuu SI-järjestelmän perussuureista pituuteen ja aikaan käytettäessä laser-anemometriaa. Tässä tutkimuksessa esitetään vaihtoehtoinen menetelmä ilman virtausnopeusmittauksen jäljitettävyysketjun rakentamiseksi. Kun tuulitunnelissa virtaavaa ilmaa kostutetaan massavirraltaan tunnetulla vesivirtauksella, pystytään ilman virtausnopeus lausumaan kostutukseen käytetyn veden massavirran funktiona ja kytkemään mittaustulos massan ja ajan kansallisten mittanormaalien kautta näiden suureiden määritelmiin. Menetelmää tutkittiin vertaamalla sen antamia ilman virtausnopeuksia Pitot-putkella mitattuihin nopeuksiin MIKESin tuulitunnelissa.

Lämpötilastabiloinnista huolimatta tutkittavassa nestenäytteessä esiintyy aina pystysuoria lämpötilagradientteja. Nämä gradientit aiheuttavat nesteeseen tiheyseroja. Mitattaessa nesteen tiheyttä areometrilla, lämpötilagradientit vaikuttavat nesteen areometriin kohdistamaan nosteeseen ja sitä kautta mittaustulokseen. Tutkimuksessa kehitettiin menetelmä, jonka avulla lämpötilagradientit voidaan ottaa huomioon ja siten pienentää tuloksen epävarmuutta. Menetelmän toimivuutta tutkittiin kokeellisesti MIKESin areometrien kalibrointilaitteistossa. Sen avulla pystytään parantamaan esimerkiksi virtausyksiköiden muunnoksen tarkkuutta massavirrasta tilavuusvirtaan.

Tässä työssä esitetyillä malleilla ja menetelmillä pystytään parantamaan virtausmetrologiassa käytettyjen mittanormaalien tarkkuutta. Menetelmä ilman virtausnopeuden mittauksen jäljitettävyyden luomiseksi massan ja ajan kansallisiin mittanormaaleihin tarjoaa laser-anemometria edullisemman ratkaisun.

Asiasanat Virtausmetrologia, termodynamiikka, kaasun massavirta, ilman virtausnopeus, nesteen tiheys

ISBN (painettu) 978-952-5610-48-2	ISSN (painettu) 1235-2704
ISBN (pdf) 978-952-5610-49-9	ISSN (pdf) 1797-9730
Kieli Englanti	Sivumäärä 84 s. + julkaisut 46 s.
Julkaisija Mittatekniikan keskus	
Painetun väitöskirjan jakelu Mittatekniikan keskus	
☒ Luettavissa verkossa osoitteessa http://lib.tkk.fi/Diss/2009/isbn9789525610499/	

Preface

The research work presented in this thesis has been carried out at the Centre for Metrology and Accreditation (MIKES) during the years 2003 - 2008.

First of all, I would like to express my gratitude to my supervisor, D.Sc. (Tech) Martti Heinonen. Collaboration with him has taught me many aspects of scientific research work. I would also like to thank Professor Markku J. Lampinen and Professor Timo Siikonen for inspiring teaching and excellent lecture notes during my post-graduate studies. I am also grateful to Professor Timo Hirvi and Dr. Heikki Isotalo for offering me the opportunity to carry out the research work for this thesis.

Furthermore, I want to thank Mr. Bernhard Niederhauser from Swiss Federal Office of Metrology and Accreditation (METAS) for his contribution in Paper **I**. I also want to thank all my colleagues at MIKES, especially the people of the research group of Thermal and Mass Quantities for the encouraging and friendly atmosphere. During the writing process of the summary of this thesis, I got valuable advice and hints from D.Sc. (Tech) Björn Hemming and Ms. Virpi Korpelainen. My wife Hanna has been the key background supporter, and her influence to complete this work has been enormous. Finally, the reviewers of Papers **I** - **V** of this thesis and all the other people who have encouraged me or given me useful advice are acknowledged.

Espoo, November 2008

Sampo Sillanpää

Contents

List of publications

This thesis consists of an overview and the following publications, which are referred to in the text by their Roman numerals.

I S. Sillanpää, B. Niederhauser and M. Heinonen, Comparison of the primary low gas flow standards between MIKES and METAS, Measurement **39**, 26 - 33 (2006).

II S. Sillanpää and M. Heinonen, The varying effect of natural convection on shear stress rate on cylindrical surfaces, Experimental Thermal and Fluid Science **32**, 459 - 466 (2007).

III S. Sillanpää and M. Heinonen, The contribution of varying shear stress to the uncertainty in gravimetric gas mass flow measurements, Metrologia **45**, 249 - 255 (2008).

IV S. Sillanpää and M. Heinonen, A mixing method for traceable air velocity measurements, Measurement Science and Technology **19**, 085409 (2008).

V M. Heinonen and S. Sillanpää, The effect of density gradients on hydrometers, Measurement Science and Technology **14**, 625 - 628 (2003).

Author's contribution

The research work presented in this thesis has been carried out at MIKES during the years 2003-2008. The thesis consists of a short overview and five publications that are referred to as **I** - **V**. These publications are the results of group efforts.

The author was responsible for carrying out all measurements at MIKES, data analysis and manuscript preparation for publication **I**.

In publication **II**, the theoretical analysis of varying shear stress, elaboration of experimental tests and assessment of results was performed by the author. The author also carried out the preparation of the manuscript.

The uncertainty analysis presented in publication **III** was developed by the author in collaboration with D.Sc. (Tech) M. Heinonen. The Monte Carlo simulation, data analysis and manuscript preparation were carried out by the author.

The theory of a mixing method was developed by the author together with D.Sc. (Tech) M. Heinonen, who participated in the design of the humidity measurement set-up. The author was responsible for the design of the wind tunnel, all measurements, and data analysis together with the uncertainty calculation and preparation of the manuscript for publication **IV**.

For publication **V**, the author designed and performed all measurements and contributed to the preparation of the manuscript and data analysis.

List of abbreviations and acronyms

AFNOR	Association Française de Normalisation
ASTM	American Society for Testing and Materials
BSI	British Standards Institution
CCD	Charge-coupled device
CFD	Computational fluid dynamics
CI	Coverage interval
CL	Confidence level
CMOS	Complementary metal oxide semiconductor
DIN	Deutsches Institut für Normung
DWS	Dynamic gravimetric gas mass flow rate standard at MIKES
Gr_x	Local Grashof number
GUM	Guide to the expression of uncertainty in measurement
HCS	Hydrometer calibration system
INRIM	National Institute of Metrological Research in Italy, formerly known as IMGC
ISO	International Organization for Standardization
LDA	Laser anemometer
LPU	Law of propagation of uncertainty
MCS	Monte Carlo simulation
METAS	Swiss Federal Office of Metrology and Accreditation
MIKES	Centre for Metrology and Accreditation in Finland
MM	Mixing method
NIST	National Institute of Standards and Technology in the United States of America
NMI	National metrology institute

NMIJ	National metrology institute in Japan
NPL	National Physical Laboratory in the United Kingdom
NSL	National standards laboratory
OIML	Organisation Internationale de Métrologie Légale
Pr	Prandtl number
PTB	Physikalisch-Technische Bundesanstalt, national metrology institute of Germany
SI	Le Système international d'unités, International System of Units
WTS	Wind tunnel air velocity measurement system

List of symbols

A	Surface area
D_n	Normalized difference
d	Calibration factor; diameter
d_{ij}	Equivalence between laboratories i and j
f	Similarity variable
g	Acceleration of free fall
I	Reading of a balance
k	Coverage factor
p	Pressure
M	Number of Monte Carlo trials
m	Mass; dimensionless constant
n	Dimensionless constant
q_m	Mass flow rate
q_v	Volume flow rate
r_w	Mixing ratio
T_w	Wall temperature
T_∞	Ambient temperature
t	Temperature; time
U	Expanded uncertainty
u	Standard uncertainty; velocity along a surface
v	Air velocity
X_i	Input variable
x_i	Estimate of the input variable; x-coordinate
Y	Measurand
y	Estimate of a measurand; y-coordinate

α Conversion factor

β Coefficient of thermal expansion

γ Surface tension of liquid

η Similarity parameter

Θ Dimensionless temperature ratio

μ Absolute viscosity

ν Kinematic viscosity

ρ Density

τ_w Shear stress

ψ Stream function

List of figures

List of tables

1 Introduction

The history of flow measurement can be traced back to the time of ancient Egypt, about 3000 years ago. The irrigation of fields was an important activity for agriculture there. The first water meters were a crude type of weir installed in water channels [1]. A basis for the idea of the traceability of flow measurement can be found in the studies of the Greek mathematician Hero of Alexandria. He understood that the volume flow rate was a function of area and velocity, $q_v = Av$ [1].

In ancient Greece, a *metronomoi* was a supervisor of weights and measures at market places. Five of them worked in Athens and another five in Pireas. To make sure that the weights and measures were consistent in both cities, they needed commonly acknowledged reference standards. From these needs, the discipline of studying measurements and traceability, called metrology [2], started to develop. Based on the invention of Hero of Alexandria, the accurate measurement of fluid volume flow rate can be verified today with a traceability chain. It is an unbroken chain of comparisons with stated uncertainties, from the definition of the unit to the measurement equipment used for routine work.

The goal of sustainable development and environmental protection at economically reasonable costs increases the need for accurate and traceable measurements. A good example is the monitoring of air quality and measurement of the number of fine particles in aerosols. It has been estimated that as many as 6 % of all deaths in the area of Central Europe are caused by the pernicious impact of these fine particles [3; 4]. As a result, a more reliable data for the surrounding environment needs to be achieved. With the data analysis, the preventive activities can be allocated more precise.

To produce an accurate gas mass or volume flow rate, a widely acknowledged measurement standard is needed. In 2001, the Advisory Commission for Metrology in Finland proposed that a national standard for small gas flow rates should be developed. In February 2002, the developing project towards the realization of the standard was started at the Centre for Metrology and Accreditation (MIKES). As a result of the project, the first version of a dynamic gravimetric measurement standard (DWS) was developed.

The operating principle of the DWS is to set a gas cylinder filled with a suitable test gas on the weighing pan of a balance. The gas cylinder is connected to a pipeline with flexible tubing. During the measurement, gas flows out from the cylinder at a constant flow rate, and indications on the balance with corresponding time values are recorded. The average mass flow rate can then be calculated by dividing the gas mass loss by the time needed for gas depletion.

In the Master's thesis of the author [5], the design, implementation and preliminary testing of the DWS apparatus were studied. In the work included in this thesis, the DWS was improved to meet the requirements of the national standard for small gas flow. According to an international evaluation in November 2004, this goal was achieved and the MIKES Flow Laboratory was nominated to work as a national standards laboratory (NSL) for small gas flow and liquid density in January 2005 [6].

Themes for research for this thesis emerged during the further development of the equipment used at the MIKES Flow Laboratory. In the field of fluid flow metrology, DWS (small gas flow rate), a wind tunnel system (WTS, air velocity) and a hydrometer calibration system (HCS, liquid density) have the same type of thermodynamic problems, for example, the effect of temperature gradients during the measurement. In this thesis, the main research problem is to show that the realization of fluid flow quantities can be improved by studying the thermodynamic phenomena of each measurement standard.

To prove the international applicability of the measurement results carried out with DWS, the metrological competence study of the measurement standard has been carried out. To improve the accuracy of the measurements and the uncertainty calculation, the effect of thermal non-equilibrium between the weighed gas cylinder and ambient air has been studied.

At MIKES, the unit of mass flow rate has been taken as a base unit of fluid flow. Thus, a key problem is to show that the traceability link between the air velocity standard and the realization of mass flow rate unit can be established.

To carry out the conversion from mass flow rate to the volume flow rate or vice versa, an accurate measurement of fluid density is needed. The density measurement of liquid can be carried out with a hydrometer. Usually, the vertical temperature distribution in the liquid is not homogenous. For that reason, a method of compensating for the effect of vertical temperature gradients in the HCS calibration liquid bath will be studied.

In this thesis, section 2 defines the traceability of a measurement result. Then, a short introduction to the calculation of measurement uncertainty is given. Section 3 presents primary calibration methods for small gas flow meters, anemometers and hydrometers. These sections give the background information for observations presented in Papers **I**-**V** and reported in section 4.

In Paper **I**, a metrological competence study of DWS to meet the requirements of the national standard for small gas flow rate has been presented. The uncertainty analysis and bilateral equivalence between two primary standards based on different operating principles were studied. The theoretical model for calculating the varying effects of natural convection on shear stress rate on cylindrical surfaces and its experimental study were performed in the work reported in Paper **II**. Paper **III** includes the study of the contribution of varying shear stress to the uncertainty in

gravimetric gas mass flow rate measurements. A novel method to establish a traceability link between air velocity standards and national standards of mass and time has been presented in Paper **IV**. Also, the uncertainty estimation and validation process of the method have been presented in the paper. Paper **V** presents a mathematical model by which the effects of temperature gradients on the hydrometer reading can be compensated.

2 Traceability and measurement uncertainty

2.1 Traceability

In the International System of Units (Le Système international d'unités, SI), measurement standard is defined as a measuring instrument or reference material which is used to realize, conserve or reproduce a unit or one or more values of a quantity [2]. By comparing a measurement device against a measurement standard, the metrological properties of a measurement device are established. As a result of this comparison, called calibration, the calibration corrections or errors with the corresponding uncertainties are obtained. Thus, the calibration of a measurement device is a basic procedure to ensure the quality of the measurement result. The result is traceable if it can be related to stated references, usually national or international standards, through an unbroken chain of comparisons which all have stated uncertainties [2]. The chain of comparisons is called a traceability chain. An example of it is shown in figure 2.1, where a simplified hierarchy of measurement standards and traceability is presented.

At the top of the chain, there is the definition of the SI unit. For example, the definition of the second is: "*the duration of 9192631770 periods of the radiation corresponding to the transition between the two hyperfine levels of the ground state of the caesium 133 atom*" [7]. The kilogram is defined as *"the mass of the international prototype of the kilogram"* [7]. Primary standards are used for realizing the unit according to the definition. They are designated or widely acknowledged as having the highest metrological qualities, and their values are accepted without reference to other standards of the same quantity [2]. Secondary standards are calibrated against the primary standard of the same quantity, and are used for calibration of working standards which are in everyday use in the field.

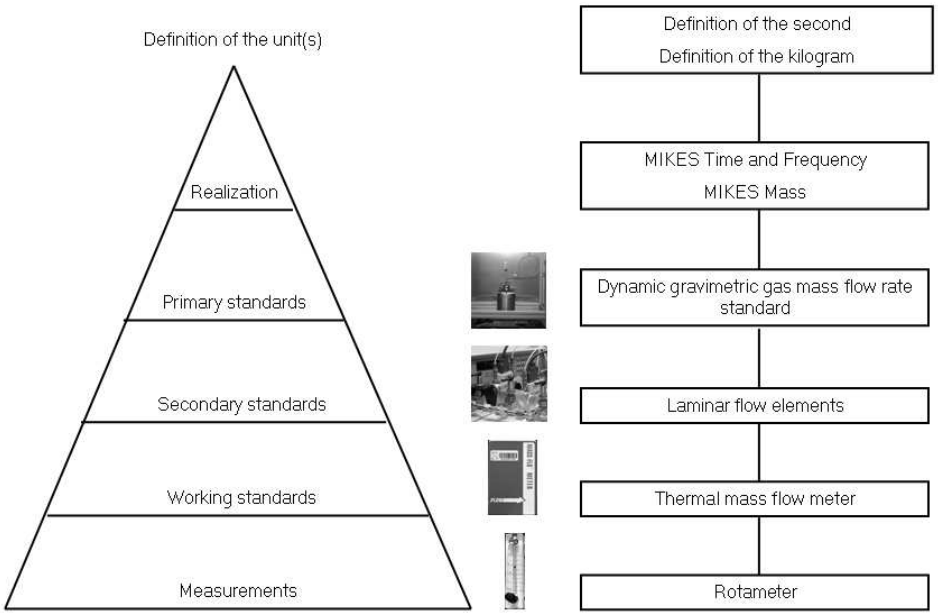

Figure 2.1: At left, the traceability chain in general, from the definition of the unit to end users, and at right, example of the chain relating to gas flow rate measurements.

A derived quantity is defined and realized with independent base quantities. For example, the velocity (m/s) is realized according to its definition in terms of the base quantities length and time. A primary standard of a derived quantity bonds it to the appropriate base quantities of SI. Thus, the traceability of a derived quantity is based on the realization of the base quantities.

2.2 Measurement uncertainty

The measurement result, after correcting all known systematic errors, is still an estimate of the value of the measurand [8]. To be useful, the measurement result should also include the uncertainty of the estimate. The uncertainty of the estimate reflects the lack of exact knowledge of the value of the measurand.

According to the Guide to the Expression of Uncertainty in Measurement (GUM), the estimate y of the measurand Y is obtained from input estimates $x_1, x_2, \ldots, x_N$ for the values of the N quantities $X_1, X_2, \ldots, X_N$. Then, the output estimate is obtained from [8]

$$y = f\left(x_1, x_2, \ldots, x_N\right). \tag{2.1}$$

The uncertainties for input estimates evaluated according to GUM are denoted by $u(x_i)$ and are called standard uncertainties. If the input estimates are assumed to be independent, the quadrature of combined standard uncertainty $u_c(y)$ is calculated as [8]

$$u_c^2\left(y\right) = \sum_{i=1}^{N} \left(\frac{\partial f}{\partial x_i}\right)^2 u^2\left(x_i\right). \tag{2.2}$$

In equation (2.2), $\partial f/\partial x_i$ is called a sensitivity coefficient. In the case of dependent (correlated) input estimates, the combined standard uncertainty is calculated as [8]

$$u_c^2\left(y\right) = \sum_{i=1}^{N} \left(\frac{\partial f}{\partial x_i}\right)^2 u^2\left(x_i\right) + 2\sum_{i=1}^{N-1}\sum_{j=i+1}^{N} \frac{\partial f}{\partial x_i}\frac{\partial f}{\partial x_j} u\left(x_i, x_j\right). \tag{2.3}$$

In equation (2.3), $u\left(x_i, x_j\right)$ is the estimated covariance of x_i and x_j.

The expanded uncertainty is obtained by multiplying the standard uncertainty by a coverage factor k. The value of the coverage factor depends on the effective degrees of freedom and desired level of confidence. If y is normally distributed, the coverage factor $k = 2$ produces a 95 % level of confidence.

GUM is currently considered the most important document in the evaluation of measurement uncertainty. Although supported by the international metrology community, ISO and many other standardization bodies, it has some limitations. For example, this can be seen by applying the GUM method to automated instruments. These instruments have embedded software with algorithms invisible to the end user. This makes the characterization of individual uncertainty components at each step very difficult or impossible [9]. Therefore other methods for measurement uncertainty evaluation, such as polynomial chaos theory [10] or unscented transform [11]

based methods, have been suggested. In accredited calibration laboratories, the derivative of GUM, EA-4/02, is in use [12].

The GUM method has been implemented in computer programs such as GUM Workbench, which is supported by the Danish Technological Institute. It has been considered handy in many practical applications [13]. In the supplement of GUM [14], the alternative numerical Monte Carlo method is presented for uncertainty calculation. This method can be used, if the GUM method is not adequate [15]; for example, if the measurement model is not exactly known.

3 Primary calibration methods for small gas flow meters, anemometers and hydrometers

3.1 Units and traceability

Units of gas mass flow rate (kg/s), gas volume flow rate (m^3/s), air velocity (m/s) and liquid density (kg/m^3) are derived from the base units of SI. Corresponding primary standards bond these derived units to the base units of mass, time and length; these are realized in Finland at MIKES [16; 17; 18]. Thus, the ultimate sources of traceability in flow measurements are from the realization of these base units. In small low-pressure gas mass and volume flow rate measurements, submultiples of units are used. Units such as mg/s, ml/min or l/min are more practical in these applications.

The concept of small gas flow can be understood to cover gas volume flow rates up to 100 l/min. In metrological applications, the velocity of moving air is from a couple of mm/s to 50 m/s and the liquid density range is from 600 kg/m^3 to 2000 kg/m^3 at temperatures between 10 °C and 40 °C [19].

3.2 Small gas flow meters

3.2.1 Methods based on mass flow rate

Mass is a property, which is independent of temperature or pressure. When measuring the mass flow rate, the use of standard temperature and pressure conditions is unnecessary. Two different gravimetric methods are used in metrology to deter-

mine the gas mass flow rate: the discontinuous static gravimetric method and the continuous dynamic gravimetric method.

In the static gravimetric method, the gas vessel is weighed before and after the flow measurement. The mass flow rate is calculated by dividing the gas mass loss by the time needed for gas depletion. The disadvantage of the method is that the vessel has to be disconnected from the measurement set-up to perform the weighing. The method has been formerly used, for example, as the national standard for small gas flow at National metrology institute in Japan (NMIJ) [20] and in an accredited calibration laboratory [21]. The expanded ($k = 2$) uncertainty of 0.1 % at mass flow rates up to 83 mg/s for the static gravimetric method has been reported in the article by Nakao et al. [20]. The static gravimetric method has also been used for the preparation of primary standard gas mixtures [22; 23; 24].

Today, most of the gravimetric systems used as the primary gas mass flow rate standards are based on dynamic weighing. This method has the advantage that more than one gravimetric comparison can be taken without removing the gas vessel from the system. The dynamic gravimetric method saves time compared to the static method, but has a challenging design problem: The flow connection from the gas vessel to the flow system prevents the bottle from being completely free from parasitic force influences as it rests on the balance. Flexible tubing can be used to limit the effect of the connection, but the gas pressure in the tube must be very stable to minimize the influence of an unstable Bourdon effect.

Dynamic gravimetric gas mass flow rate measurement systems are used in at least seven NMIs [25], and have been described in literature; for example, in Paper **I** (0.1 mg/s. . . 625 mg/s, $U = 0.8$ %. . . 0.3 %), in articles by Sillanpää and Niederhauser et al. [26; 27] (8 mg/s. . . 250 mg/s, $U = 0.2$ %), and in the paper by Knopf et al. [28] (0.5 mg/s. . . 40 mg/s, $U = 0.01$ %. . . 0.3 %). In the dynamic gravimetric method, the gas vessel filled with suitable test gas is placed on a balance as in figure 3.1. After

reaching a stable gas flow, the indications of the balance are recorded simultaneously with timer readings. The average gas mass flow rate during the measurement period is then determined, for example, as a slope of linear fitting of buoyancy corrected balance indications and time values [Paper **I**].

At MIKES, the dynamic gravimetric method provides a base for traceable gas mass flow rate measurements. With the traceability chain, the improvements in the measurement accuracy of DWS improves, for example, the measurement accuracy of the number concentration of fine particles in aerosols. The dynamic gravimetric method also provides a basis for producing traceable gas mixtures [29; 30]. These mixtures are used, for example, for calibrating air quality measurement devices or gas analyzers [31].

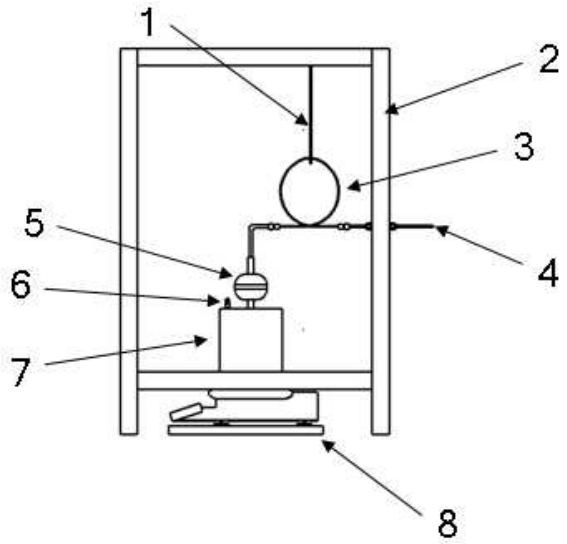

Figure 3.1: Schematic figure of dynamic gravimetric gas mass flow rate measurement standard at MIKES. 1: Connection tube hanger, 2: casing, 3: connection tube, 4: outflow, 5: pressure regulator, 6: one-way valve for filling, 7: gas vessel, 8: balance on a stone table.

3.2.2 Methods based on volume flow rate

A primary standard for volume flow rate is usually an application of a piston-cylinder assembly. Primary standards of this type are in use, for example, in the Swiss Federal Office of Metrology and Accreditation (METAS) [32] (200 ml/min. . . 20000 ml/min, $U = 0.1$ %) and in the National Institute of Metrological Research (INRIM, formerly IMGC) in Italy [33; 34; 35] (0.1 ml/min. . . 2000 ml/min, $U = 0.02$ %. . . 0.05 %). In a piston-cylinder standard, the velocity of a rising piston is determined from the length of the movement and the elapsed time. When the average velocity of the piston during the measurement period is known, the volume flow rate can be calculated assuming uniform motion of the piston and using the effective cross-sectional area of the cylinder. The obtained volume flow rate is usually converted to some standard conditions, for example, at the temperature of 273.15 K and pressure of 101325 Pa. A modified piston-cylinder assembly has also been used as a measurement standard for leak rates [36].

Static expansion systems, or $PVTt$ standards, have been used in flow metrology since the beginning of 1970s, first reported by Olsen and Baumgarten [37]. In this method, gas flow is determined using a technique in which a steady flow is diverted into a nearly empty collection tank with a known volume during a measured time interval. The average gas temperature and pressure in the tank are measured before and after the filling process. These measurements are used to determine the density change in the collection volume attributed to the filling process. In principle, the mass flow rate can be determined by multiplying the density change by the collection vessel volume, and dividing the result by the collection time. The method was developed further by Wright [38] and Johnson et al. [39; 40] (1 l/min. . . 2000 l/min, $U = 0.02$ %. . . 0.05 %). A very small gas flow rate version, down to 0.01 mg/min, was developed by Nakao [41] (0.01 mg/min. . . 5 mg/min, $U = 0.0001$ %. . . 0.2 %).

3.3 Anemometers

3.3.1 Pressure difference based methods

The operating principle of the Pitot tube was first discovered by French hydraulic engineer Henri de Pitot in 1732 [42]. A Pitot tube is made up of two concentric tubes. The inner tube is open, and the annular space between the tubes is sealed at one end (see figure 3.2). The band of small, radial holes through the wall of the outer tube is located about eight outer tube diameters from the sealed end. The tubes are set parallel to the direction of the flow with the sealed end facing into the flow [43]. The other ends of the tubes are connected to the differential pressure gauge between the inner tube and the annular space. The inner tube senses both the static and dynamic pressures due to the motion of the fluid. The radial holes sense only the static pressure. The measured differential pressure is due only to the motion of the fluid, and the speed of the fluid flow can be calculated from the equation

$$v = \sqrt{\frac{2\Delta p}{\rho}}, \tag{3.1}$$

where Δp and ρ are the differential pressure between the parallel tubes and the density of flowing fluid, respectively.

The uncertainty of the Pitot tube at lower fluid flow velocities is dominated by the differential pressure measurement. For that reason, the usable lower velocity limit for a Pitot tube is around 2 m/s. Below that velocity, the uncertainty of the differential pressure measurement is too large.

Before the adoption of the laser anemometer (LDA), the Pitot tube was considered to be the primary standard instrument for air speed measurement at national standards laboratories [44; 45] (0.5 m/s. . . 50 m/s, $U = 20\ \%. . . 0.4\ \%$, $k = 3$). With the Pitot tube, the traceability of air velocity measurement can be traced back to the primary realization of units of mass, length, time and temperature.

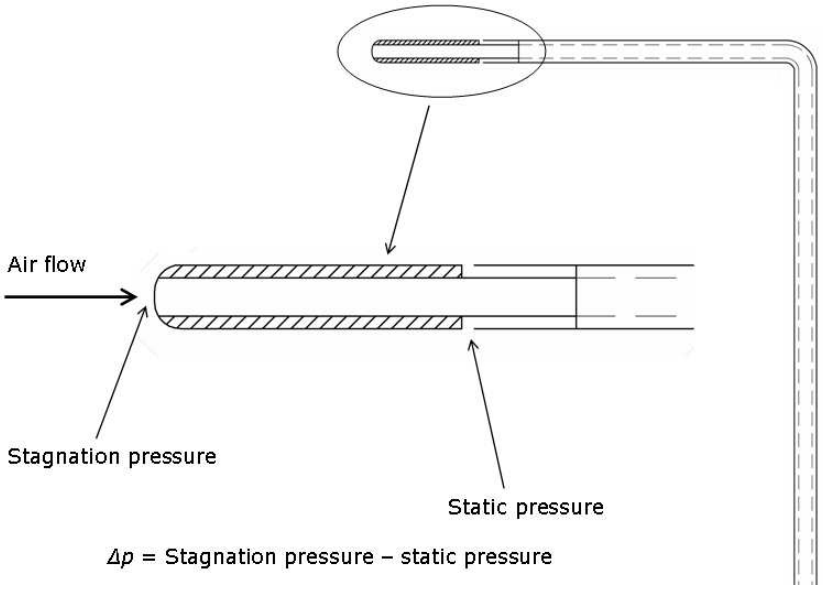

Figure 3.2: Schematic figure of a Pitot tube.

3.3.2 Light scattering based methods

The measurement technique of laser anemometry is presented in figure 3.3. In its simplest form, it is based on splitting a laser beam into two separate beams and then coupling them through a small intersection angle. The coherence of the two beams in the intersection forms an interference pattern. The distance between the bright bands in the pattern can be calculated from

$$d = \frac{\lambda}{2\sin\left(\frac{\theta}{2}\right)}, \tag{3.2}$$

where λ and θ are the wavelength of the laser light and the angle between the two beams, respectively. The distance d is called as the calibration factor of the LDA system. The intersection of the two beams is the test volume of the system. When small particles inserted into the fluid pass through the test volume, they reflect light. The average flow velocity at the test volume can then be calculated by dividing d by the average frequency of detected reflections [46; 47].

Nowadays, LDA is the most commonly used primary measurement method for air velocity in metrological wind tunnels at many NMIs [46; 48] and accredited laboratories [49]. The traceability link between the air velocity measurement and the SI base units of length and time can be built using a light scattering particle on the rim of a disk with known radius and circumferential speed. By calculating the linear speed of the particle, the calibration factor of LDA can be determined [46]. With LDA based measurement techniques, expanded uncertainties such as 0.006 m/s can be achieved even at very low flow velocities [46]. However, Pitot tubes together with thermal anemometers are still used as transfer standards in inter-laboratory comparisons [50] and as reference standards in accredited laboratories.

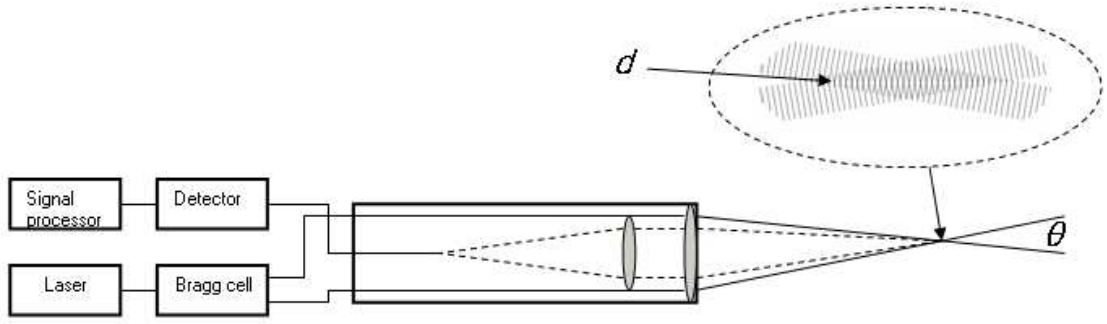

Figure 3.3: Operating principle of a laser anemometer.

3.3.3 Other methods

Various methods based on different operating principles are presented in the literature. They are mostly used for calibration of thermal anemometers at low fluid velocities, or in particular operation conditions.

Measurement standards at low air velocities are based on mechanical systems which, for example, drive the anemometer at a desired constant speed [51] (measurement

range 0 m/s...0.15 m/s, expanded uncertainty $U = 4.1$ %) and [52] (0 m/s...0.350 m/s, $U = 0.001$ m/s). Standards can be also based on different techniques generating a laminar velocity profile in a pipe [53] (0 m/s...2.9 m/s, $U = 1.5$ %) and [54] (0.1 m/s...0.9 m/s, $U = 0.02$ m/s).

In the method suggested by Elgerts and Adams [55], a vibrating piston in a cylinder produces a reference velocity field for an orifice plate placed at the opposite end of the cylinder. The apparatus is used for calibrating thermal anemometers in oscillating flow in the velocity range from 0.2 m/s to 2.3 m/s. The result of the calibration is a dynamic Nusselt number with an expanded uncertainty of 12 %.

3.4 Hydrometers

3.4.1 Constant mass hydrometer

According to Archimedes' law, the mass of liquid displaced by a freely floating hydrometer is equal to the mass of the hydrometer, if surface tension is assumed to be negligible [56]. Hydrometers can be divided into constant volume and constant mass hydrometers. By putting appropriate weights on the constant volume hydrometer, it is adjusted to float up to a specific mark in liquids with different densities. The constant mass hydrometer (see figure 3.4) floats at different heights in the liquid, and its mass is not changed by weights during normal use. In this thesis, only the constant mass hydrometers are considered, because they are now more widely used, and their specifications and measurement procedures are well documented by the International Organization for Standardization (ISO) [57; 58; 59; 60; 61], Organisation Internationale de Métrologie Légale (OIML) [62], Association Française de Normalisation (AFNOR) [63], American Society for Testing and Materials (ASTM) [64; 65; 66; 67], British Standards Institution (BSI) [68; 69; 70; 71] and Deutsches Institut für Normung (DIN) [72; 73; 74].

Figure 3.4: Constant mass hydrometer.

Hydrometers are widely used, for example, in refuelling aircrafts. The fuel supplier is interested in the volume of the fluid, but the airline needs the net weight of the fuel to calculate the take-off weight of the aircraft.

3.4.2 Cuckow's method

Cuckow's calibration method for hydrometers was initially developed at the National Physical Laboratory (NPL) in the United Kingdom by Cuckow [75]. In this method, a hydrometer is first weighed in air. Then it is submerged to the required level and its apparent mass is measured in the liquid of known density. The reference density value is calculated from the difference in the weighing results in air and in the reference liquid. The density of the reference liquid can be measured by hydrostatic weighing of a body of a known volume [19].

Various implementations of the method exist. Different calibration liquids such as n-nonane, petroleum and ethanol are in use, and a variety of techniques adjusting the hydrometer to the desired scale mark are exploited. The adjustment can be done by lowering or raising the hydrometer or the liquid surface [76]. The alignment of the hydrometer in Cuckow's method can be automated by taking advantage of machine vision applications based on the charge-coupled (CCD) or complementary metal oxide semiconductor (CMOS) [77; 78; 79] cells. For Cuckow's method, the best reported expanded ($k = 2$) relative calibration uncertainty is $24{\cdot}10^{-6}$ [80].

3.4.3 Other methods

Although Cuckow's method is the most commonly used and the most accurate multi-point calibration method for hydrometers [80], other methods, like the direct comparison method and the ring method [81; 82], are in use at some laboratories. In the direct comparison method, the calibrated hydrometer is immersed in the calibration liquid together with the reference hydrometer, and the readings are compared. The ring method consists of finding the position on the scale, with possible additional weights, where the hydrometer freely floats in a liquid of known density and surface tension. If the apparent mass of the hydrometer, body diameter and the distance from the freely floating point are known, the reference value for any other point on the scale can be calculated. The disadvantage of the method is that hydrometers with different scales need various calibration liquids with different densities, because they have to be able to float freely.

4 Thermodynamic studies of primary standards in flow metrology

4.1 Metrological competence study of the MIKES dynamic gravimetric gas mass flow rate standard (Paper I)

4.1.1 Metrological competence study

The traceability of a measurement result consists of an unbroken chain of comparisons with stated uncertainties, from the definition of the unit to the measurement device used, use of documented and generally accepted measurement procedures, and personnel with adequate professional skills. The metrological competence of a laboratory includes the professional skills of the personnel and the sufficient metrological performance of measurement standards.

The metrological competence study can be carried out by comparing two primary measurement standards in different NSLs. This inter-comparison on a transfer standard allows evaluating metrological performance of the primary standard in both laboratories, and the equivalence of the calibration methods and services. In addition, the creditability of the traceability chain and the uncertainty estimation can be studied.

The metrological competence study with data analysis of the MIKES dynamic gravimetric gas mass flow rate measurement standard is presented in Paper **I**. The study was carried out by arranging a bilateral comparison with the Swiss Federal Office of Metrology and Accreditation (METAS). In the study, the results of the MIKES dynamic gravimetric gas mass flow rate measurement system were compared against the volumetric standard based on a piston-cylinder assembly at METAS. A good

quality commercial transfer standard based on laminar flow elements having good short-term stability was used. The calibration measurements were first carried out at MIKES and then the transfer standard was transferred to METAS. After the measurements, the standard was shipped back to MIKES and calibration measurements were repeated.

4.1.2 Analysis of the results of a bilateral comparison between MIKES and METAS

The comparison results were analyzed according to the outlines presented in articles by Cox [83; 84]. The equivalence between two laboratories at each measurement point was calculated as

$$d_{ij} = \Delta q_{ri} - \Delta q_{rj}, \tag{4.1}$$

where Δq_r is the relative difference between the reference and transfer standard. Subscripts i and j refer to measurements carried out at MIKES and METAS, respectively. The associated expanded uncertainty is $U(d_{ij}) = 2u\,(d_{ij})$, where

$$u^2\,(d_{ij}) = u^2\,(\Delta q_{ri}) + u^2\,(\Delta q_{rj})\,. \tag{4.2}$$

The normalized difference is

$$D_n = d_{ij}/U(d_{ij}). \tag{4.3}$$

Table 4.1 presents the relative differences between the reference and transfer standards at MIKES and METAS in percents, the degrees of equivalence and their expanded uncertainties in percents, and the normalized differences. The parameters of MIKES were calculated from the second calibration set only, because the analysis showed that the uncertainty of the flow control with needle valves and its effect on the measurement result was larger than assumed. At MIKES and METAS, each comparison point was measured four times, and the average relative difference was used as a result. The maximum relative difference between the laboratories was

1.3 % at the mass flow rate of 0.42 mg/s, as can be seen also from figure 4.1. For the second calibration set at MIKES, the needle valves were replaced by thermal mass flow controllers.

Table 4.1: The results of the comparison in the flow range from 0.42 mg/s to 625 mg/s.

Flow / (mg/s)	Δq_r (MIKES) / %	Δq_r (METAS) / %	d_{ij} / %	$U(d_{ij})$ / %	D_n
0.42	0.22	0.27	-0.05	0.36	-0.13
2.1	-0.14	-0.05	-0.09	0.34	-0.28
6.3	-0.06	-0.04	-0.02	0.25	-0.07
10.4	0.04	-0.02	0.06	0.25	0.22
14.6	0.03	0.00	0.03	0.25	0.09
18.8	-0.07	0.00	-0.08	0.25	-0.31
20.8	-0.02	-0.02	0.00	0.25	0.00
41.7	-0.16	-0.21	0.05	0.25	0.20
125	0.03	-0.09	0.12	0.25	0.49
250	0.01	-0.01	0.02	0.28	0.06
377	0.01	0.02	-0.02	0.28	-0.04
500	-0.03	0.00	-0.03	0.28	-0.12
625	-0.28	-0.13	-0.15	0.28	-0.53

A rule of thumb for analyzing the results was presented in [85]. The comparison results between the two laboratories are acceptable, if the normalized difference fulfils $|D_{ni}| < 0.5 \quad \forall \; D_{ni}, \quad i = 1 \ldots \mathrm{N}$, where N is the number of comparison points. It means that the independent results from similar measurements made at the two laboratories can be expected to agree to within d_{ij} with a 95 % confidence interval. The rule usually estimates the 95 % confidence interval correctly, but can underestimate it in some cases. In this comparison, the above presented criteria is exceeded only at one measurement point, 625 mg/s, and only slightly.

The analysis showed that the improved flow control produced results which were more congruent with results obtained in the recognized NSL. After the improvement, the uncertainty calculations performed at MIKES were tenable. In addition, the mathematical measurement model and the calculation method for measurement

results were correct. The largest uncertainty sources seemed to be the stability of a balance indication, time measurement and the parasitic effect of the connecting tube.

In the study presented in Paper **I**, the mass and volume flow rate based primary standards were compared. The results of the study showed that these two methods are comparable and equal in realizing small gas flows. This agrees with the results reported by Niederhauser and Barbe [27].

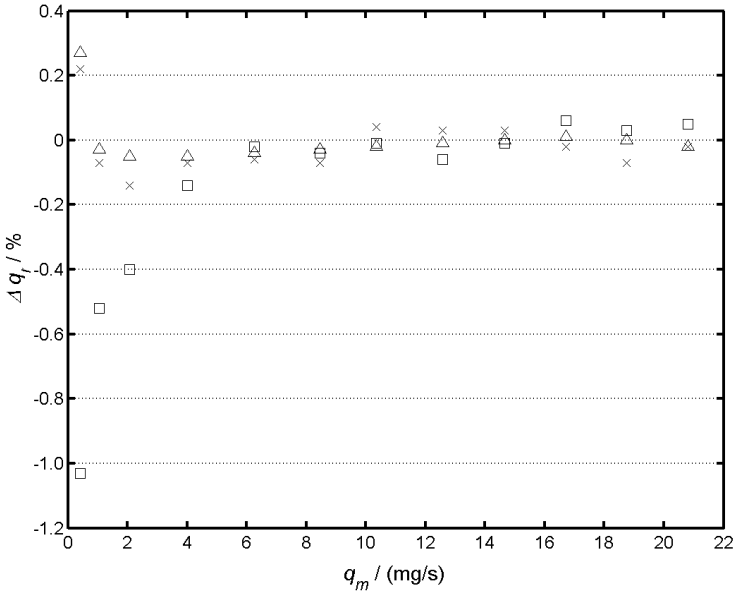

Figure 4.1: Relative difference between the reference and the transfer standard (Δq_r) measured at points (q_m) from 0.42 mg/s to 20.8 mg/s. □: MIKES April 2003, △: METAS May 2003, ×: MIKES June 2003.

4.2 Method for estimating the varying shear stress rate induced by natural convection flow on cylindrical surfaces (Paper II)

4.2.1 Drag

The force resisting the movement of a solid object through a liquid or gas is called drag. It is the sum of all aerodynamic or hydrodynamic forces in the direction of movement. Three types of drag can be categorized: parasitic, lift-induced and wave drag [86]. In this study, the parasitic drag is in focus, because lift-induced and wave drag appear on wing profiles and flow velocities near the speed of sound, respectively.

Parasitic drag consists of skin friction, pressure drag and interference drag. Because very low fluid flow velocities are studied here, the latter two are assumed to be negligible. Thus, skin friction is the only component of parasitic drag, and it is due to shear stresses in the boundary layer [87].

4.2.2 Shear stress induced by natural convection

In a dynamic gravimetric gas mass flow rate measurement, a thermal non-equilibrium between a weighed gas cylinder and ambient air cannot be prevented. The non-equilibrium causes heat transfer between ambient air and the weighed object. If the heat transfer is based on natural convection, a flow field upward or downward around the object arises. This natural convection flow originates when a body force acts on a fluid containing density gradients. The net effect is a buoyancy force, which drives the fluid motion. In this study, density gradients are assumed to originate from temperature gradients, and gravity is the body force.

Assuming that there is no slip on the wall (i.e., the fluid velocity on the wall is zero). Then, for a Newtonian fluid, the shearing stress on the wall and the rate of shearing strain (the velocity gradient) can be linked together with

$$\tau_w = \mu \left. \frac{du}{dy} \right|_w , \tag{4.4}$$

where τ_w, μ and du/dy are the shear stress on the wall, absolute viscosity and velocity gradient, respectively.

The first scientific study of flow field due to natural convection was presented by Schmidt et al. [88]. And in metrology, the effect of shear stress induced by natural convection was studied widely by Gläser et al. [89; 90; 91]. The convection effect was illustrated and studied experimentally with the method proposed by Matilla et al. [92] and Tian et al. [93]. The method was based on infrared thermal imaging. The convective motion has been studied numerically, first in two-dimensional cavities having different aspect ratios, and later in three dimensional boxes filled with different gases or liquids [94; 95]. The first study about convective forces using computational fluid dynamics (CFD) code was reported by Mana et al. [96]. The stability of natural convection flow along a vertical plate has been studied by direct numerical simulation by Aberra et al [97]. For a steady state solution, a lattice Boltzmann based algorithm has been proposed in the paper by Zhou et al. [98].

In Paper **II**, the method for estimating the net effect of time-dependent, varying shear stress rate driven by natural convection flow on cylindrical surfaces was developed. The method is based on the numerical similarity solution of laminar boundary layer equations.

The idea of a boundary layer was first presented by Prandtl in 1904 [99]. His work was based on the equations first presented by Navier [100] and Stokes [101]. Prandtl's idea was to divide the velocity field into two areas: the boundary layer and the area outside it. In the boundary layer, the viscosity is dominant, whereas

outside it, the viscosity can be neglected without significant effect on the velocity field (see figure 4.2). By taking into account the Boussinesq approximation (see, for example, [102; 103; 104]), the basic equations for a laminar boundary layer driven by natural convection are

$$\frac{\partial u}{\partial x}+\frac{\partial v}{\partial y}=0, \tag{4.5}$$

$$u\frac{\partial u}{\partial x}+v\frac{\partial u}{\partial y}=g\beta\left(\Delta T\right)+\frac{\partial^2 u}{\partial y^2}, \tag{4.6}$$

$$u\frac{\partial T}{\partial x}+v\frac{\partial T}{\partial y}=\alpha\frac{\partial^2 T}{\partial y^2}. \tag{4.7}$$

Here, u is the velocity component along the plate and v is normal to it. The buoyancy parameter $g\beta$ depends on the fluid ($\beta=\left(d\rho_a/dT\right)/\rho_a$), whereas the thermal diffusivity $\alpha=k/\left(\rho c_p\right)$ is assumed to be constant. $\Delta T=T_w-T_\infty$ which is the temperature difference between the plate and ambient air. ν is kinematic viscosity.

The similarity solution of equations (4.5) to (4.7) was first presented by Schmidt et al. [88] and developed further for arbitrary geometry by Pop and Takhar [105]. The idea of the solution is to introduce at first a similarity parameter

$$\eta=\left(\frac{\mathrm{Gr}_x}{4}\right)^{\frac{1}{4}}\frac{y}{x}\qquad \mathrm{Gr}_x=\frac{\beta g\left(T_w-T_\infty\right)x^3}{\nu^2}, \tag{4.8}$$

where Gr_x is a local Grashof number. Next, the stream function is defined as

$$\psi\left(x,y\right)=f\left(\eta\right)\left[4\nu\left(\frac{\mathrm{Gr}_x}{4}\right)^{\frac{1}{4}}\right]. \tag{4.9}$$

To satisfy the continuity equation exactly, it has to be set

$$u=\frac{\partial\psi}{\partial y}\qquad v=-\frac{\partial\psi}{\partial x}. \tag{4.10}$$

After differentiation, the velocity components u and v are

$$u=2\left(x\beta g\left(T_w-T_\infty\right)\right)^{\frac{1}{2}}f'\left(\eta\right) \tag{4.11}$$

$$v=\left[\frac{\beta g\left(T_w-T_\infty\right)\nu^2}{4x}\right]^{\frac{1}{4}}\left(\eta f'\left(\eta\right)-3f\left(\eta\right)\right), \tag{4.12}$$

where a prime indicates differentiation with respect to η. When the dimensionless temperature difference is defined as follows

$$\Theta = \frac{T - T_\infty}{T_w - T_\infty}, \tag{4.13}$$

the similarity variables reduce the system of partial differential equations to the two non-linear differential equations

$$f''' + (3 + m + n)\, f f'' - 2\,(1 + m + n)\, f'^2 + \Theta = 0, \tag{4.14}$$

$$\Theta'' + (3 + m + n)\,\mathrm{Pr} f \Theta' - 4\mathrm{mPr} f' \Theta = 0. \tag{4.15}$$

In equations (4.14) and (4.15), f, m, n, Θ and Pr are the similarity parameter, constants relating to the heat transfer and geometry, dimensionless temperature ratio and Prandtl number, respectively. The detailed description about the transformation process from equations (4.5) through (4.7) to equations (4.14) and (4.15) can be found, for example, from [88]. The first numerical solution for equations (4.14) and (4.15) was given by Ostrah [106]. The shear stress can now be expressed with similarity variables, when the flow field around the surface of the cylinder is known and the fluid is to be assumed Newtonian

$$\tau_w = \rho\nu \frac{du}{dy} = \frac{2\mu}{x} \left[x\beta g\,(T_w - T_\infty)\right]^{\frac{1}{2}} \left(\frac{Gr_x}{4}\right)^{\frac{1}{4}} f''(0)\,. \tag{4.16}$$

The shear stress rate is a function of temperature difference, and the temperature difference is a function of time. It is shown in Paper **II** that the effect of the average shear stress affecting the surface at some arbitrary time interval from $t' \ldots t$ can be calculated as a time average of instantaneous shear stresses

$$\overline{\Delta\tau_w} = \frac{1}{t - t'} \int_{t'}^{t} \tau_w\,(\Delta T\,(t))\, dt, \tag{4.17}$$

where τ_w is calculated with the equation (4.16). With the proposed calculation method and an appropriate surface temperature measurement of the cylindrical object, it is possible to estimate the flow field around it, as presented in figure 4.3. The method was studied experimentally by using a balance and measuring the surface temperature of the gas cylinder in the DWS with a thermistor or thermal imager.

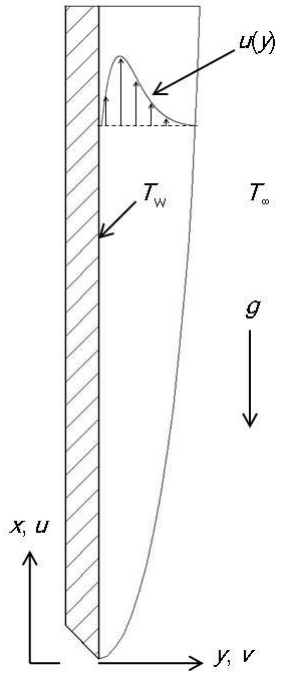

Figure 4.2: Development of boundary layer on a vertical plate, $T_w > T_\infty$.

Three measurement cycles were performed with the heated cylinder. In cycles 1 and 3, the wall temperature of the cylinder as a function of time was monitored every two seconds with a small thermistor attached on the wall. In cycle number 2, the thermistor was detached and the wall temperature was observed with a thermal imager. Concurrently with the temperature measurements, the indication of the balance was recorded to find out the corresponding shear stress rate. The results of the comparison between the theory and experiments are presented in figure 4.4. Based on the comparison, the assumption of zero pressure and interference drag seems to be realistic. Figure 4.5 illustrates an interesting finding from the theoretical study: the horizontal arrangement of the cylindrical object will reduce the effect of shear stress.

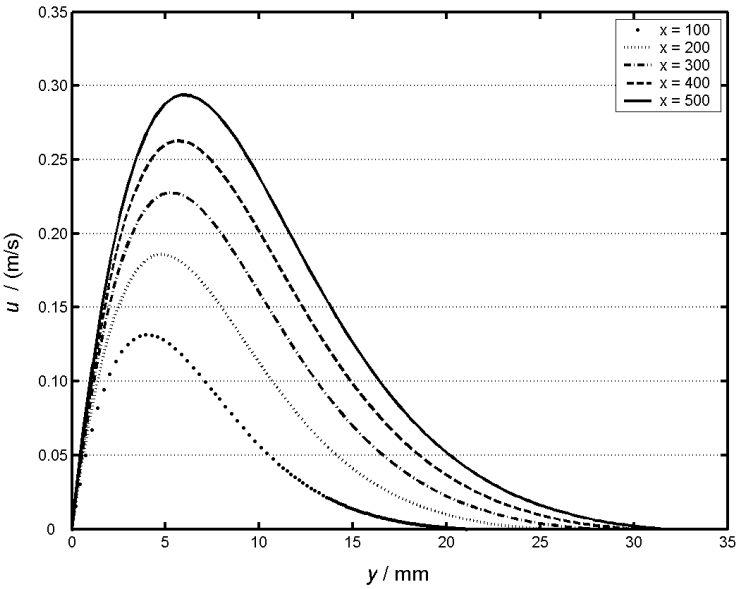

Figure 4.3: Example of calculated velocity profiles for the vertical gas cylinder at a temperature difference of 10 K at different distances from the leading edge. Small ticks: $x = 100$ mm, dotted line: $x = 200$ mm, dash-dot line: $x = 300$ mm, dashed line: $x = 400$ mm and solid line: $x = 500$ mm.

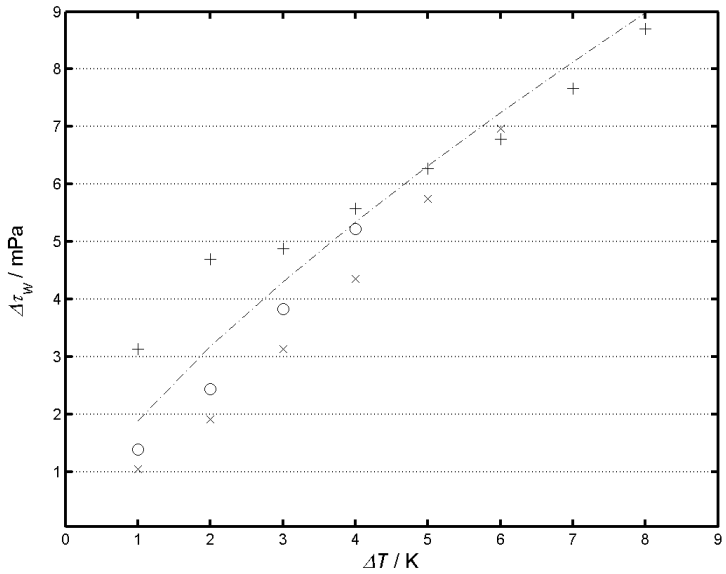

Figure 4.4: Measurement results and theoretical curve for the vertical gas cylinder. +: measurement 1, ∘: measurement 2, ×: measurement 3. Dash-dot line: theoretical curve.

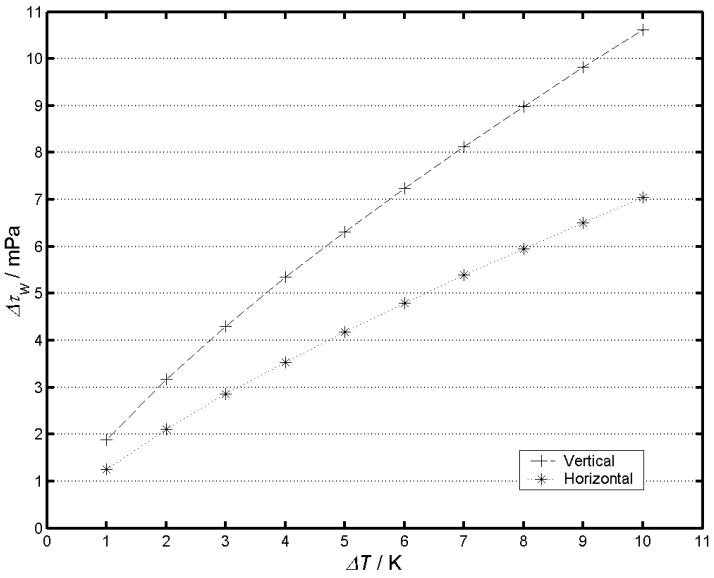

Figure 4.5: Theoretical effect of natural convection. $+$: vertical, $*$: horizontal gas cylinder.

4.3 Contribution of varying shear stress to the uncertainty in gravimetric gas mass flow rate measurements (Paper III)

4.3.1 Measurement model and uncertainty

In Paper **II**, equation (4.17) was used for estimating the effect of varying shear stress. From this equation, the effect on the balance indication of a gravimetric gas mass flow rate standard can be obtained. By integrating equation (4.17) with regard to the surface area of a gas cylinder and differentiating it, the following equation is obtained

$$\delta\dot{m}_C = \frac{d}{dt}\frac{1}{g}\int \overline{\Delta\tau_w}\, dA, \tag{4.18}$$

where $\delta\dot{m}_C$ is the effect of shear stress due to natural convection.

In the DWS at MIKES, the gas mass flow rate is determined continuously recording the indications of a balance and their corresponding time values. The mass flow rate is then calculated by a slope of linear fitting of air buoyancy corrected balance indications and corresponding time values. The measurement process is modeled with the equation

$$\dot{m}_t = \beta\left(\dot{I} - \delta\dot{I} - \frac{m_t}{\rho_t}\dot{\rho}_a - \frac{m_t\rho_a}{\rho_t^2}\dot{\rho}_t - \delta\dot{m}_T - \delta\dot{m}_C - \delta\dot{m}_L\right), \tag{4.19}$$

where m_t, I, δI, ρ_t, ρ_a, δm_T, δm_C and δm_L are the true mass of the gas cylinder, indication of the balance, errors due to balance mechanics, effective density of the gas cylinder, density of ambient air, effect of the connecting tube, effect of shear stress due to natural convection and leakage out of the system, respectively. $\beta = (\alpha\,(1-\rho_a/\rho_t))^{-1}$, where $\alpha = (1-\rho_{a0}/\rho_r)^{-1}$, $\rho_{a0} = 1.2$ kg/m^3 and $\rho_r = 8000$ kg/m^3. Dots indicate differentiation with time.

For the calculation of the measurement result including uncertainty, the following discrete approximation is used

$$\dot{m}_t \approx \frac{\beta}{\Delta t}\left(\Delta I - \Delta\delta I - m_t\Delta\rho_a/\rho_t - m_t\Delta\rho_t\rho_a/\rho_t^2 - \Delta\delta m_T - \Delta\delta m_C - \Delta\delta m_L\right). \tag{4.20}$$

For uncertainty calculation, a more detailed description of components $\{\Delta I \ldots \Delta\delta m_L\}$ is presented in table 4.2. Assuming that the components are independent of each other, the combined standard uncertainty can be calculated with equation (2.2).

Table 4.2: Uncertainty components

i	x_i	Unit	Annotation
1	ΔI	kg	Gas mass difference, including contributions due to balance nonlinearity and a standard deviation of the mean of the difference between the linear fit of the balance indications and the instantaneous indication of the balance
2	$\Delta\delta I$	kg	Resolution of the balance and its stability
3	ρ_a	kg/m^3	Air density
4	$\Delta\rho_a$	kg/m^3	Air density change during the measurement
5	ρ_t	kg/m^3	Density of the gas cylinder
6	$\Delta\rho_t$	kg/m^3	Density change of the gas cylinder during the measurement
7	Δt	s	Error in time measurement
8	$\Delta\delta m_T$	kg	Effect of connection tube during the measurement
9	$\Delta\delta m_C$	kg	Effect of natural convection during the measurement
10	$\Delta\delta m_L$	kg	Leakage out of the system during the measurement

4.3.2 Effect of varying shear stress on the uncertainty

During the dynamic gravimetric weighing process, parasitic forces such as δm_T and δm_C affect the indication of a balance. Also, forces generated by ambient conditions, such as the density of air (buoyancy), electrostatic forces, condensation and thermal gradients and, in the case of ferromagnetic materials, magnetic forces, may

affect the measurement result [89]. Buoyancy can be estimated by calculating the density of surrounding air according to equations presented first by Giacomo [107] and then specified twice by Davis [108] and Picard et al. [109]. Local gravitational, electrostatic and possible magnetic forces can be assumed constant during the measurement, and therefore neglected. The condensation of water is prevented by ensuring that the measurement is conducted above the dew-point temperature.

Paper **III** presents the effect of convective forces (temperature gradients) on the uncertainty in dynamic gravimetric gas mass flow rate measurement. Four test cases were studied. The uncertainty calculation including the theory presented in Paper **II** was implemented as a MATLAB-code. In the first case, the temperature difference model between the gas vessel and ambient air presented in figure 4.6 was used. This model gave a temperature difference of 1 K at the maximum. The effect of varying shear stress was calculated according to equation (4.18). The measurement uncertainty was evaluated by using equation (4.20) as a measurement model. The second case was similar to the first one, except the temperature difference was now as stable as possible. In that model, the maximum temperature difference was 0.2 K. The third and fourth cases were similar to the first and second ones, except the effect of shear stress was not taken into account in the uncertainty calculation ($\Delta\delta m_C = 0$). In these two last cases, variations in temperature were only taken into account by calculating the buoyancy correction to the indications of the balance. Table 4.3 gives a summary of results of the combined standard uncertainties for the studied test cases at four mass flow rates from 0.1 mg/s to 625 mg/s. As can be seen, at the larger gas mass flow rates the effect of varying shear stress was almost negligible. By comparing cases one and three at the gas mass flow rate of 0.1 mg/s, the combined standard uncertainty was over 3.75 times larger in case one than in case three. This shows that the effect of varying shear stress has to be taken into account in uncertainty evaluation, especially for smaller gas mass flow rates.

Table 4.3: Summary of combined standard uncertainties in four studied test cases.

	625 mg/s	321 mg/s	21 mg/s	0.1 mg/s
Case	u_c / %	u_c / %	u_c / %	u_c / %
1	0.12	0.11	0.08	0.49
2	0.12	0.10	0.07	0.17
3	0.12	0.10	0.07	0.13
4	0.12	0.10	0.07	0.13

Figures 4.7 and 4.8 show the relative distribution of uncertainty components at two gas mass flow rates: 0.1 mg/s and 625 mg/s. The numerical values of contributions with four significant digits can be found in tables 4 and 5 in Paper **III**. If the contribution of any component in the tables is smaller than 0.005 %, it has been marked as 0.00. From the figures, it can be seen that the uncertainty due to natural convection flow dominates at the mass flow rate of 0.1 mg/s, if the temperature change during the measurement is large. Otherwise, the most significant component is the effect of the connecting tube.

Table 4.4: Comparison of the uncertainty calculation methods at gas mass flow rate of 0.1 mg/s for the DWS.

Method	y / (mg/s)	$u(y)$ / (mg/s)	95 % CL or CI / (mg/s)
LPU	0.0969	0.0005	$[0.0959, 0.0979]$
MCS	0.0970	0.0005	$[0.0961, 0.0979]$

Equation (2.2) is based on the assumption of independent uncertainty components. The air temperature measurement at the boundary layer of a gas cylinder is used for calculating both the shear stress on the cylinder wall and the buoyancy correction of the indication of the balance. To show that using the same temperature distribution

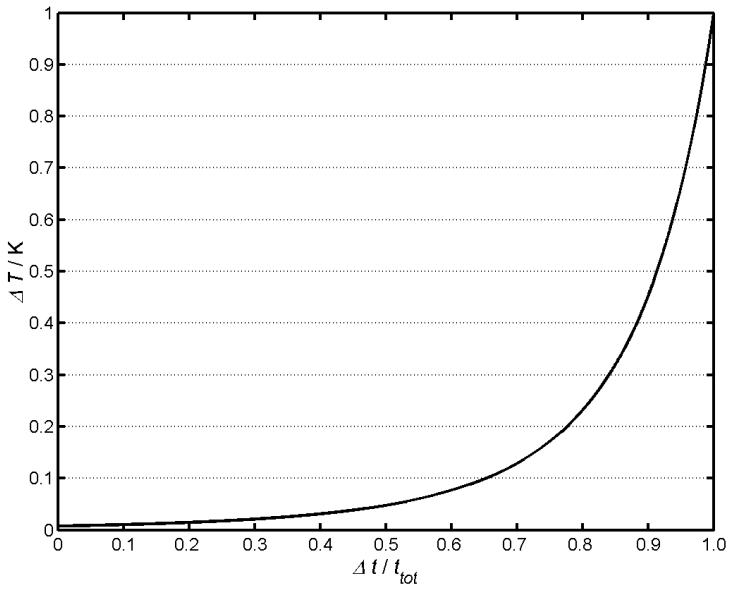

Figure 4.6: Temperature difference model between the wall of the gas cylinder and ambient air as a function of dimensionless measurement time. The model was used for simulating a situation, where the temperature of the gas vessel or ambient air increases or decreases during a measurement cycle.

for both purposes will not have an effect on the combined standard uncertainty, the calculation was carried out numerically (MCS) according to the ISO guidelines [14]. The gas mass flow rate of 0.1 mg/s was chosen, because at this flow rate the effect of varying shear stress was found to be the most significant. During the MCS, the number of trials $M = 10^4$ and each temperature value from the model in figure 4.6 was assumed to be normally distributed. The probability density function is shown in figure 4.9, where 95 % coverage interval (CI) is marked with vertical dotted lines. In table 4.4, results obtained analytically (LPU) and numerically (MCS) for the gravimetric gas mass flow rate standard DWS are compared, and 95 % confidence level (CL) or coverage interval (CI) are presented. Figure 4.9 shows the normal distribution of the output estimate y. The results of the comparison showed a good agreement between the LPU and MCS methods. From this can be concluded that using the same temperature difference model for calculating both the shear stress and the buoyancy correction will not have a notable effect on the combined standard uncertainty.

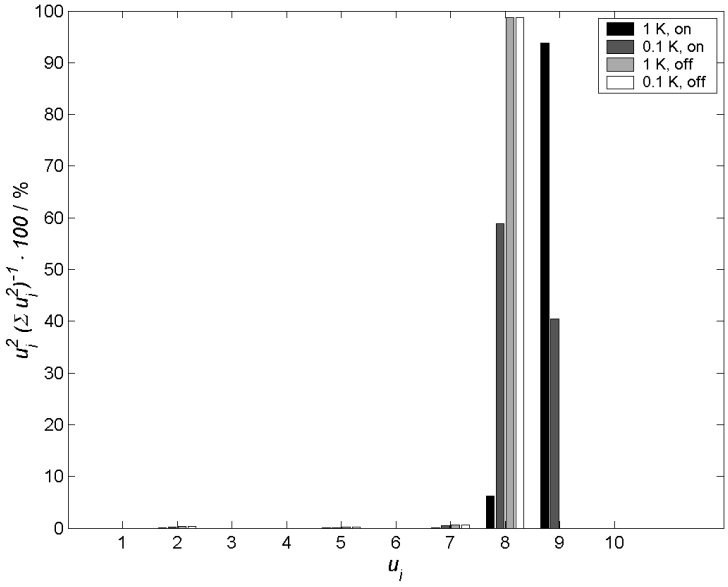

Figure 4.7: Comparison of the contribution of different uncertainty components to the combined standard uncertainty at mass flow rate 0.1 mg/s. Numbers on the x - axis refer to the numbering of uncertainty components in table 4.2. Numbers 8 and 9 correspond the effect of the connecting tube and the effect of natural convection, respectively.

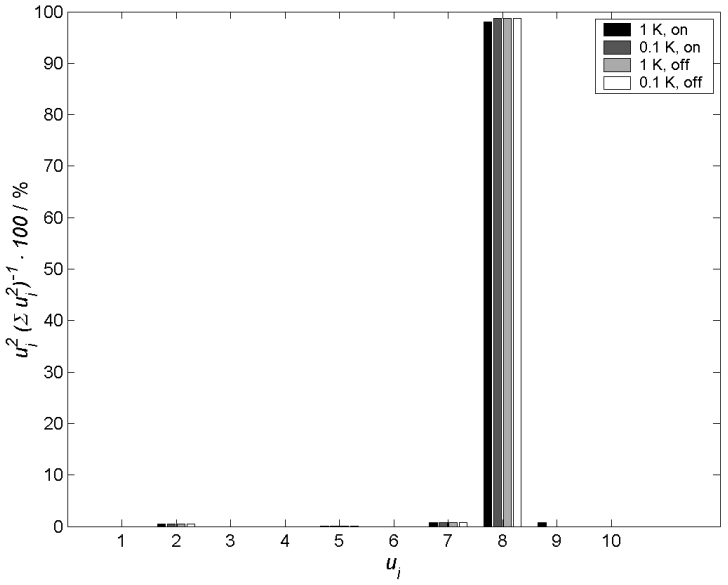

Figure 4.8: Comparison of the contribution of different uncertainty components to the combined standard uncertainty at mass flow rate 625 mg/s. Numbers on the x - axis refer to the numbering of uncertainty components in table 4.2. Numbers 8 and 9 correspond the effect of the connecting tube and the effect of natural convection, respectively.

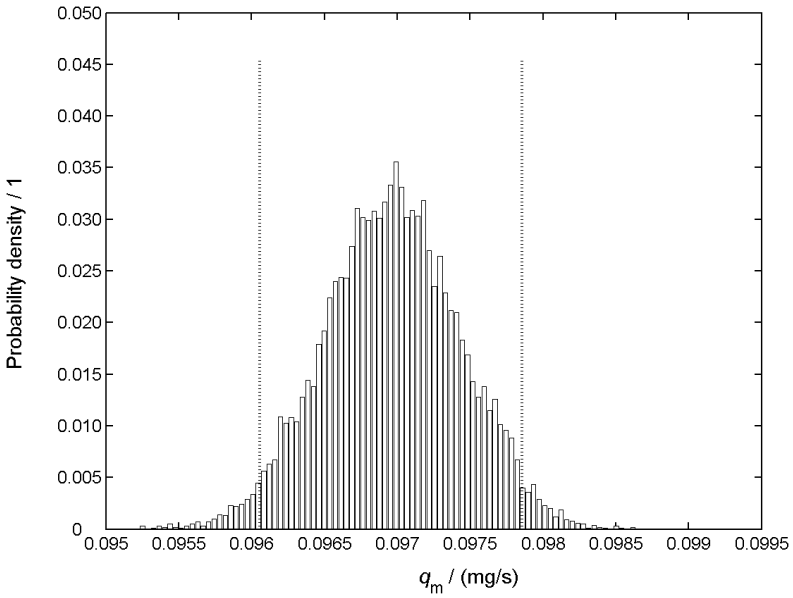

Figure 4.9: The probability density function of the output quantity at M = 10^4 values of Y at the gas mass flow rate of 0.1 mg/s.

4.4 Novel method for linking air velocity to the national standards of mass and time (Paper IV)

4.4.1 Mixing method

In Paper **IV**, a new mixing method (MM) is proposed for linking air velocity to the national standards of mass and time. Instead of establishing different primary standards for different flow quantities, gravimetric mass flow standards are used as the primary source of traceability in the whole gas metrology field at MIKES. A mixing method was developed for creating a traceability link to air velocity measurements.

When humidifying air in the wind tunnel with a constant mass flow rate, the humidity of air in the test section is directly proportional to the air velocity. It is calculated as

$$v_3 = \frac{\dot{m}_{v2}}{\rho_{a3} A_3} \left[\frac{(r_{w1} + 1)}{\Delta r_w} + 1 \right], \tag{4.21}$$

where A_3, r_{w1} and Δr_w are the cross section area of the test section, the mixing ratio (ratio of water vapour and dry air) of incoming air $r_w = \dot{m}_v / \dot{m}_a$ and the mixing ratio difference between the air inlet and the test section $\Delta r_w = r_{w3} - r_{w1}$, respectively. Numbers in subscripts refer to the locations in the wind tunnel as specified in figure 4.10.

4.4.2 Application of the mixing method at MIKES

MM was applied to an open-circuit wind tunnel at MIKES. The design of the tunnel was based on the rules of thumb presented by Mehta et al. [110]. The shape of the contraction is a sixth-order polynomial, based on the study of Laine and Harjumäki [111]. The exit diffuser was designed exploiting the experimental test results and CFD-simulation, reported in papers by Bell and Mehta [112] and Gullman-Strand et al. [113], respectively.

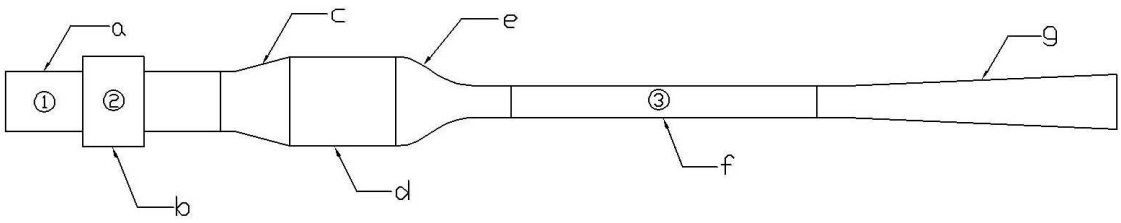

Figure 4.10: Schematic drawing of the MIKES wind tunnel. a: humidification unit, b: blower, c: wide angle diffuser, d: settling chamber, e: contraction, f: test section, g: exit diffuser. The humidification process of air: 1: mixing of feed water vapour and make-up air, 2: dilution of components in the blower, 3: air flow with homogeneous mixing ratio.

In the MIKES system, the mass flow rate of evaporated water is determined with a dynamic gravimetric method. The mixing ratio is measured indirectly with a dew-point hygrometer and barometer. The water vapour pressure is calculated from the dew-point temperature using Sonntag's formula [114]. Near the laboratory conditions (t = 20 °C, ϕ = 50 %), the water vapour is assumed to obey the ideal gas law. Then, the mixing ratio can be presented as a function of total barometric pressure and partial pressure of water

$$r_w = \frac{M_w}{M_a}\frac{p_v}{p_a} \approx 0.6220\frac{p_v}{p - p_v}, \tag{4.22}$$

where the molar masses of water $M_w = 18.015$ g/mol [115] and air $M_a = 28.964$ g/mol [115] are assumed to be constants.

A Pitot tube installed at the centreline of the test section was used for studying the performance of the MM at four measurement points in the air velocity range from 5.5 m/s to 30 m/s. At each point, the measurements were repeated three times. The average results are presented in table 4.5. Air velocity values measured at the centreline of the test section were used as the indication of the Pitot tube. It is shown in Paper **IV** that the maximum non-uniformity of the velocity profile is less than 1.5 %. The non-uniformity was taken into account in the measurement uncertainty of the Pitot tube. The maximum difference between the methods was

0.7 % at the velocity of 5.5 m/s. The difference was smaller than 0.5 % elsewhere. Based on the results, the MM seems to be feasible in the studied flow range.

Table 4.5: Comparison of air velocities measured by the mixing method (MM) and Pitot tube.

MM / (m/s)	U ($k = 2$) / (m/s)	Pitot / (m/s)	U ($k = 2$) (m/s)	MM - Pitot / (m/s)	MM - Pitot / %
5.50	0.2	5.46	0.7	0.04	0.7
10.3	0.4	10.3	1.1	0.00	0.0
21.1	0.8	21.0	2.2	0.07	0.3
29.3	1.6	29.2	3.1	0.13	0.4

4.5 Effect of temperature gradients on the indication of hydrometers (Paper V)

4.5.1 Measurement procedure

When measuring the density of liquid with a hydrometer, temperature gradients at the immersion depth in the liquid will affect the measurement result. In the study presented in Paper **V**, a method for compensating for the effect of temperature gradients on the hydrometer reading was developed.

The study was carried out using the MIKES hydrometer calibration system (HCS), which is based on Cuckow's method. A detailed description of the HCS can be found in publications by Heinonen [116] or by Lorefice et al. [76]. The range the hydrometer used was from 1950 kg/m^3 to 2000 kg/m^3, with a scale division of 0.5 kg/m^3 to ensure a proper immersion without additional weights to the ethanol bath.

The effect of temperature gradients in the ethanol bath of HCS was studied by changing the liquid level with respect to the top of the jacketed glass vessel in two calibration sets. In both sets, the five calibration points were measured twice. In the first calibration set, the ethanol surface was about 60 mm above the liquid surface in the jacket, to produce a significant vertical temperature gradient in the liquid. For the second calibration set, the ethanol surface was dropped about 7 mm below the liquid surface in the jacket, to minimize the temperature gradient. The vertical temperature distribution in the liquid was measured in both sets at ten points using two small Pt-100 probes of a digital thermometer. Each point was measured four times. The temperature in the bath was set to 15 °C and ambient temperature was 25 °C. A comparison of the vertical temperature profiles in the ethanol is presented in figure 4.11. The maximum temperature gradient in the first calibration set was

0.05 K/mm, producing a significant density gradient located near the liquid surface.

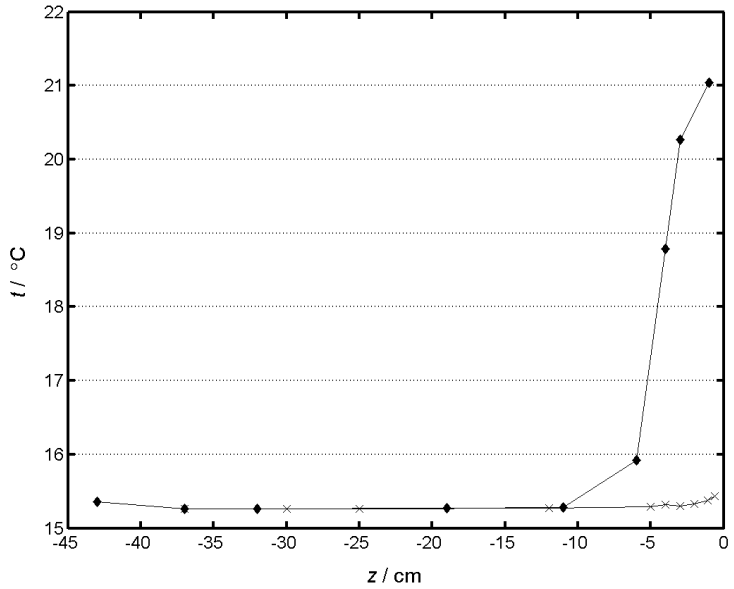

Figure 4.11: The measured vertical temperature distributions in the HCS in the two cases. Distances are measured from the surface of liquid. ♦: first calibration set, ×: second calibration set.

4.5.2 Compensation for the effect of density gradients

It is assumed in Paper **V** that there are only vertical density gradients in the liquid, and that the hydrometer is symmetrical with respect to its vertical axis. The correction due to non-uniform density can be estimated by

$$\delta F_b \approx \frac{\pi g \Delta z}{4} \sum_{i=1}^{n} \left[\rho_l\left(z_i\right) - \rho_{l0}\right] d_h^2\left(z_i\right), \tag{4.23}$$

where $d_h(z_i)$, $\rho_l(z_i)$ and ρ_{l0} are the diameter of the hydrometer, actual liquid density at a point z_i and bulk density of the liquid, respectively. The idea of the method is to determine the net correction to the buoyancy force due to the density gradients.

By taking into account δF_b, the equation for the density value in Cuckow's method is

$$\rho_x = \rho_a + \frac{(\rho_l - \rho_a)\left[I_a\left(1-\frac{\rho_a}{\rho_r}\right)+\frac{\pi d\gamma_x}{g}\right][1+\beta(T-T_r)]}{I_a\left(1-\frac{\rho_a}{\rho_r}\right)-I_l\left(1-\frac{\rho'_a}{\rho_r}\right)-\frac{\delta F_b}{g}+\frac{\pi d\gamma_l}{g}}. \tag{4.24}$$

In equation (4.24), ρ'_a, ρ_l, I_a, I_l γ_l γ_x, d, T, T_r and β are density of air during weighing in liquid, density of the calibration liquid, balance indication when weighing the hydrometer in air and in liquid, surface tension of the calibration liquid, surface tension of the liquid in which the hydrometer is normally used, stem diameter of the hydrometer at the meniscus level, temperature of the liquid, reference temperature and cubic thermal expansion coefficient of the hydrometer material, respectively. The reference density of ethanol was determined with hydrostatic weighing and was checked against the equation presented in the article by Bettin et al. [117].

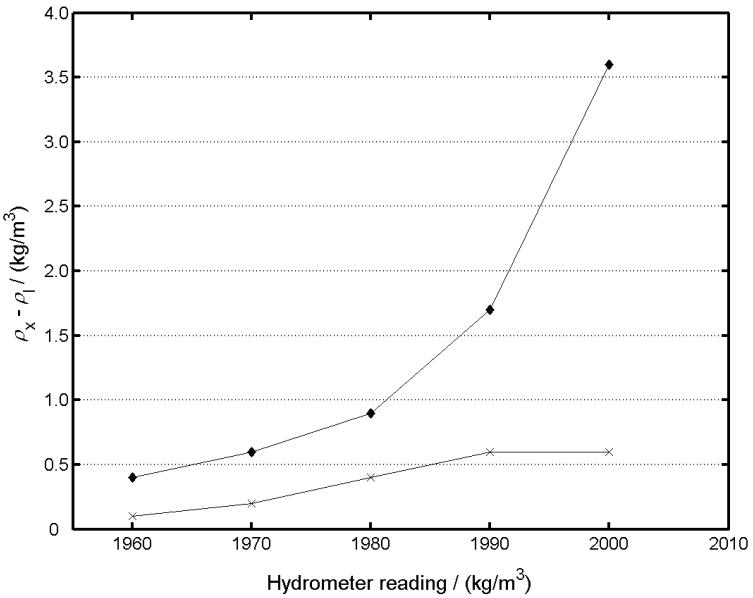

Figure 4.12: Calibration results without density gradient correction (ρ_x = reference density, ρ_L = indication of the hydrometer) ♦: first calibration set, ×: second calibration set.

The results of the first calibration set with larger density gradients and without the correction according to the equation (4.23) are compared to the results obtained

from the second set in figure 4.12. In figure 4.13 calibration results are re-calculated using equation (4.24). As can be seen from the results, the difference between the two calibration sets is now less than a scale division of the hydrometer.

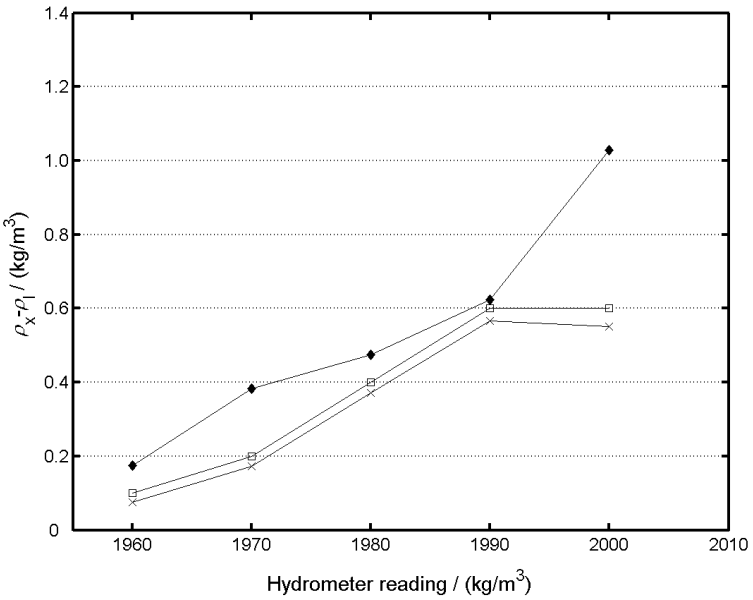

Figure 4.13: Re-calculated calibration results (ρ_x = reference density, ρ_L = indication of the hydrometer) ♦: first calibration set, ×: second calibration set, □: original results from the second set.

With the developed method, it is possible to compensate for the effect of vertical temperature gradients on the hydrometer reading. However, to carry out the compensation properly, vertical temperature gradients have to be measured with very short steps.

5 Discussion and conclusions

A metrological competence study of the MIKES dynamic gravimetric gas mass flow rate standard to meet the requirements of the national measurement standard was carried out. The obtained results proved the international equivalence of the DWS and confirmed that the uncertainty calculations are realistic. This has been shown in Paper **I**.

A mathematical model for describing the average force due to the time-dependent varying shear stress driven by natural convection flow on cylindrical surfaces was developed in Paper **II**. Based on this model, the improved measurement model for DWS and the effect of the force on the combined standard uncertainty was presented in Paper **III**.

The results of the work reported in Paper **III** showed that the rapid changes of shear stress due to temperature variation during a measurement cycle cannot be ignored, and should be included in the uncertainty budget of a dynamic gravimetric gas mass flow rate standard. When the equilibrium between the weighed gas cylinder and ambient air was disturbed, the shear stress variation was one of the three most dominating uncertainty components in the uncertainty budget at gas mass flow rate 0.1 mg/s. The theoretical and experimental studies carried out in this thesis showed that the presented theoretical model was an adequate tool for estimating the varying shear stress on cylindrical surfaces.

Papers **I** - **III** proved that the results from two primary calibration methods based on the realization of mass and volume flow rates were comparable. The standard measurement uncertainty of the DWS at MIKES is a little bit higher than in other NSLs. However, by exploiting the results from Papers **I** - **III**, the calculation methods for the measurement result and combined standard uncertainty of DWS are excellent.

A mixing method gives a novel and less expensive way to link the air velocity calibrations to the SI base units of mass and time. The method presented in Paper **IV** is suitable for a Pitot tube calibration in a wind tunnel at flow velocities from 5 m/s to 30 m/s. A disadvantage of the method is that it is sensitive to changes in the ambient mixing ratio difference. The humidification affects air temperature. To improve the accuracy of the results, a dew-point hygrometer was used instead of capacitive sensors.

A mathematical method for compensating for the effect of density gradients in the liquid on the measurement result of a hydrometer was developed in the study presented in Paper **V**. The obtained results showed that the method can be used for improving the quality of hydrometer measurements and calibrations. Also, it can be exploited for estimating the uncertainty related to temperature gradients and density gradients in general. The improved accuracy of the liquid density measurement reduces the uncertainty of conversion from volume flow rate to mass flow rate, or vice versa.

Results of this thesis include a collection of new mathematical models and a new measurement method. The first model can be used for a more accurate assesment of the impact of varying natural convection flow on the weighed gas cylinder wall and its contribution to the combined standard uncertainty of the dynamic gravimetric gas mass flow rate standard. The second model describes correction to the indication of a hydrometer, if vertical density gradients are present in the liquid. The mixing method gives a novel and less expensive way to establish the traceability link from air velocity measurement to the national standards of mass and time, instead of length and time.

The results presented in this thesis improve the accuracy of the realization of fluid flow units. Both mathematical models are already implemented as a part of the DWS and HCS measurement systems at MIKES. DWS with the improvements pre-

sented in this thesis has been already used for calibrating of instruments used for air quality monitoring. Topics for future research could include a time-dependent CFD-simulation of the dynamic gravimetric system to improve the calculation accuracy of the effect of varying shear stress. With a laser anemometer, the potential of the MM will be clarified even at air velocities less than 5 m/s. By refining the evaporation process to be more stable and developing the mixing of vapour and air, the uncertainty of the method could be improved. In addition, the use of a psychrometer instead of a dew-point hygrometer would reduce the cost of implementation of the MM.

References

[1] R. S. Medlock. June 1986. The historical development of flow metering. Measurement + Control, pages 11–22.

[2] BIPM, IEC, IFCC, ISO, IUPAC, IUPAP, and OIML. 1993. International vocabulary of basic and general terms in metrology.

[3] N. Künzli, R. Kaiser, S. Medina, M. Studnicka, O. Chanel, P. Filliger, M. Herry, F. Jr. Horak, V. Puybonnieux-Texier, P. Quénel, J. Schneider, R. Seethaler, J.-C. Vergnaud, and H. Sommer. 2000. Public-health impact of outdoor and traffic-related air pollution: a European assessment. The Lancet 356, pages 795–801.

[4] J. Pekkanen. 2004. Kaupunki-ilman pienhiukkasten terveysvaikutukset. Duodecim 120, pages 1645–1652. In Finnish.

[5] S. Sillanpää. 2003. Design, implementation and testing the calibration equipment for small gas flow meters. Master's thesis, Helsinki University of technology. In Finnish.

[6] Päätös kansallisen mittanormaalilaboratorion nimeämisestä. 2005. Technical Report Dnro 13/71/2005, MIKES. In Finnish.

[7] Bureau International des Poids et Mesures (BIPM). 2006. The international system of units.

[8] BIPM, IEC, IFCC, ISO, IUPAC, IUPAP, and OIML. 1993. Guide to the expression of uncertainty in measurement.

[9] J. Wirandi, A. Lauber, and W. J. Kulesza. 2006. Problem of applying modern uncertainty concepts to the measurement of instrument-specific parameters. IEEE Transactions on Instrumentation and Measurement 55, pages 700–705.

[10] T. E. Lovet, F. Ponci, and A. Monti. 2006. A Polynomial chaos approach to measurement uncertainty. IEEE Transactions on Instrumentation and Measurement 55, pages 729–736.

[11] L. Angrisani, M. D'Apuzzo, and R. S. Lo Moriello. 2006. Problem of applying modern uncertainty concepts to the measurement of instrument-specific parameters. IEEE Transactions on Instrumentation and Measurement 55, pages 737–743.

[12] European co-operation for Accreditation. 1999. Expression of the uncertainty of measurement in calibration.

[13] W. C. Losinger. 2004. A review of GUM workbench. The Americal Statistician 28, pages 165–167.

[14] BIPM, IEC, IFCC, ISO, IUPAC, IUPAP, and OIML. 2004. Guide to the expression of uncertainty in measurement - Supplement 1: Numerical methods for the propagation of distributions.

[15] M. G. Cox and B. R. L. Siebert. 2006. The use of a Monte Carlo method for evaluating uncertainty and expanded uncertainty. Metrologia 43, pages S178–S188.

[16] H. Kajastie, K. K. Nummila, A. Rautiainen, K. Riski, and A. Satrapinski. 2008. Loss measurements on superconducting Nb by a cryogenic dual compensated calorimeter for the implementation of the kilogram standard by the levitation mass method. Metrologia 45, pages 68–74.

[17] K. Kalliomäki and T. Mansten. 2005. Short and Long Term Stability of Kvarz Hydrogen Masers CH1-76 and CH1-75A. In: Proceedings of 2005 EFTF Meeting,. Besançon, France.

[18] M. Merimaa, K. Nyholm, M. Vainio, and A. Lassila. 2007. Traceability of laser frequency calibrations at MIKES. IEEE Transactions on Instrumentation and Measurement 56, pages 500–504.

[19] S. V. Gupta. 2002. Practical density measurement and hydrometry. Institute of Physics. ISBN 0-7503-0847-8.

[20] S. Nakao, Y. Yokoi, and M. Takamoto. 1997. Development of a calibration facility for small mass flow rates of gas and the uncertainty of a sonic venturi transfer standard. Flow Measurement and Instrumentation 7, pages 77–83.

[21] M. Bair. 1999. The dissemination of gravimetric gas flow measurements through an LFE calibration chain. In: NCSL workshop and symposium. Charlotte NC USA.

[22] M. J. T. Milton, P. T. Woods, and P. E. Holland. 2002. Uncertainty reduction due to correlation effects in weighing during the preparation of primary gas standards. Metrologia 39, pages 97–99.

[23] A. Alink and A. M. H. van der Veen. 2000. Uncertainty calculations for the preparation of primary gas mixtures. Metrologia 37, pages 641–650.

[24] A. Alink. 2000. The first key comparison of primary standard gas mixtures. Metrologia 37, pages 35–49.

[25] J. D. Wright. 2003. What is the ”best” transfer standard for gas flow? In: FLOMEKO 2003, 12-14 May.

[26] S. Sillanpää and M. Heinonen. 2003. The MIKES measuring system for gas mass flow. In: FLOMEKO 2003, 12-14 May.

[27] B. Niederhauser and J. Barbe. 2002. Bilateral comparison of primary low-gas-flow standards between the BNM-LNE and METAS. Metrologia 39, pages 573–578.

[28] D. Knopf and W. Richter. 1998. Highly accurate calibration gas mixtures by dynamic-gravimetric preparation. PTB-Mitteilungen 108, pages 201–203.

[29] D. Knopf. 2001. Continuous dynamic-gravimetric preparation of calibration gas mixtures for air pollution measurements. Accreditation and Quality Assurance 6, pages 113–119.

[30] J. Barbe, J. Couette, J.-M. Picault, and A. Marschal. 2001. Traceability of standard gas mixtures prepared by the dynamic gravimetric method. Bulletin du Bureau National de Métrologie 120.

[31] D. Knopf, J. Barbe, W. Richter, and A. Marschal. 2001. Comparison of the gas mass flow calibration systems of the BNM-LNE and the PTB. Metrologia 38, pages 197–202.

[32] B. Niederhauser. 2001. Swiss primary volumetric standard for low gas flows: experiences and progress. In: Métrologie 22.-25. October. France.

[33] R. F. Berg and G. Cignolo. 2003. NISTŰIMGC comparison of gas flows below one litre per minute. Metrologia 40, pages 154–158.

[34] G. Cignolo, F. Alasia, A. Capelli, R. Goria, and G. La Piana. 2005. A primary standard piston prover for measurement of very small gas flows: an update. Sensor Review 25, pages 40–45.

[35] M. Bergoglio, G. Raiteri, G. Rumiano, and W. Jitschin. 2006. Intercomparison of gas flow-rate measurements at IMGC, Italy, and UASG, Germany, in the range from 10^{-8} to 10^{-3} Pa m^3/s. Vacuum 80, pages 561–567.

[36] W. Jitschin, U. Weber, and H.K. Hartmann. 1995. Convenient primary gas flow meter. Vacuum 46, pages 821–824.

[37] L. Olsen and G. Baumgarten. 1971. Gas Flow Measurement by Collection Time and Density in a Constant Volume. In: Flow: Its Measurement and Control in Science and Industry, pages 1287–1295. Instrument Society of America.

[38] J. D. Wright. 2003. Gas flow measurement and standards; development and validation of a $PVTt$ primary gas flow standard. Ph.D. thesis, Kogakuin University.

[39] A. N. Johnson, J.D. Wright, M.R. Moldover, and P. I. Espina. 2003. Temperature Characterization in the Collection Tank of the NIST 26 m^3 $PVTt$ Gas Flow Standard. Metrologia 40, pages 211–216.

[40] J.D. Wright, A. N. Johnson, M. R. Moldover, and G. M. Kline. 2003. Gas Flowmeter Calibrations with the 34 L and 677 L $PVTt$ Standards. Technical Report 250-63, National Institute of Standards and Technology.

[41] S. Nakao. 2006. Development of the $PVTt$ system for very low gas flow rates. Flow Measurement and Instrumentation 17, pages 193–200.

[42] R. P. Benedict. 1984. Fundamentals of temperature, pressure and flow measurement. John Wiley and Sons. ISBN 0-471-89383-8.

[43] R. Klopfenstein Jr. 1998. Air velocity and flow measurement using a Pitot tube. ISA Transactions 37, pages 257–263.

[44] P. Bradshaw. 1969. Experimental fluid mechanics. Pergamon Press.

[45] N. E. Mease, W. G. Jr. Cleveland, G. E. Mattingly, and J.M. Hall. 1992. Calibrations at the National Institute of Standards and Technology. In: Proceedings ot the 1992 Measurement Science Conference. Anaheim, California, USA.

[46] V. E. Bean and J. M. Hall. 1999. New primary standard for air speed measurement at NIST. In: Proceedings of the NCSL workshop and symposium.

[47] V. Iyer and M. Woodmansee. 2005. Uncertainty analysis of laser-Doppler-velocimetry measurements in a swirling flowfield. AIAA Journal 43, pages 512–519.

[48] N. Kurihara, Y. Terao, S. Nakao, and M. Takamoto. 1999. Development and uncertainty analysis of a laser Doppler velocimeter calibrator for the flow velocity standard. Transactions of the Japan Society of Mechanical Engineers B 65, pages 3029–3034.

[49] J. R. Sanches, H. Müller, I. Care, Y. Cordier-Duperray, and J. M. Seynhaeve. 2004. Air velocity sensors' intercomparison using LDA as standards. In: Proceedings of the 12. International symposium on Applications of Laser Techniques to Fluid Mechanics. Lisbon, Portugal.

[50] J. M. Hall, V. E. Bean, and G. E. Mattingly. 1999. Preliminary results from interlaboratory comparisons of air speed measurements between 0.3 m/s and 15 m/s. In: Proceedings of the NCSL workshop and symposium.

[51] A. Al-Garni. 2007. Low speed calibration of hot-wire anemometers. Flow Measurement and Instrumentation 18, pages 95–98.

[52] L. Chua, H-S. Li, and H. Zhang. 2000. Calibration of hot wire for low speed measurements. International Communications in Heat and Mass Transfer 27, pages 507–516.

[53] Z. Yue and G. Malmström. 1998. A simple method for low-speed hot-wire anemometer calibration. Measurement Science and Technology 9, pages 1506–1510.

[54] T. Lee and R. Budwig. 1991. Two improved methods for low-speed hot-wire calibration. Measurement Science and Technology 2, pages 643–646.

[55] D. Elgerts and R. Adams. 1989. Dynamic hot-wire anemometer calibration using an oscillating flow. Journal of Physics E: Scientific Instruments 22, pages 166–172.

[56] H. Wagenbrecht, W. Gorski, and A. Kozdon. 1985. Ein verbessertes Prüfverfahren für Normalaräometer. PTB-Mitteilungen 95, pages 322–326.

[57] ISO. 1981. ISO 649-1: Laboratory glassware; density hydrometers for general purposes; specifications.

[58] ISO. 1981. ISO 649-2: Laboratory glassware; density hydrometers for general purposes; test methods and use.

[59] ISO. 1987. ISO 387: Hydrometers; principles of construction and standardisation.

[60] ISO. 1998. ISO 3675: Crude petroleum and liquid petroleum products; laboratory determination of density; hydrometer method.

[61] ISO. 1979. ISO 4801: Glass alcoholometers and alcohol hydrometers not incorporating a thermometer.

[62] OIML. 1985. OIML R44: Alcoholometers and alcohol hydrometers and thermometers for use in alcoholometry.

[63] NF. 1983. NF B 35-311: General use density hydrometers.

[64] ASTM. 2005. ASTM E-100: Standard specification for ASTM hydrometers.

[65] ASTM. 2005. ASTM E-126: Standard test method for inspection and verification of hydrometers.

[66] ASTM. 2005. ASTM D-1298-99: Standard method for density, relative density (specific gravity) or API gravity of crude petroleum and liquid petroleum products by hydrometer method.

[67] ASTM. 2004. ASTM D-891-95: Standard test method for specific gravity, apparent, of liquid industrial chemicals.

[68] BS. 1991. BS 718: Specification for density hydrometers.

[69] BS. 1973. BS 734-1: Measurement of the density of milk using a hydrometer. Specification for hydrometers for use in milk.

[70] BS. 1959. BS 734-2: Measurement of the density of milk using a hydrometer. Methods.

[71] BS. 1962. BS 734C: Measurement of the density of milk using a hydrometer. Percentage of total solids and non-fatty solids in milk corresponding to given fat content and observed density fat content range 2Ű6 per cent (with fat in the liquid state).

[72] DIN. 1981. DIN 12791-1: Laboratory glassware; density hydrometers; general requirements.

[73] DIN. 1978. DIN 12791-2: Laboratory glassware; density hydrometers, standard sizes, designations.

[74] DIN. 1983. DIN 12791-3: Laboratory glassware; density hydrometers; use and test methods.

[75] F. W. Cuckow. 1949. A new method of high accuracy for the calibration of reference standard hydrometers. Journal of Society of Chemical Industry 68, pages 44–49.

[76] S. Lorefice, M. Heinonen, and T. Madec. 2000. Bilateral comparisons of hydrometer calibrations between the IMGC-LNE and the IMGC-MIKES. Metrologia 37, pages 141–147.

[77] Y. J. Lee, K. H. Chang, J. C. Chon, and C. Y. Oh. 2004. Automatic alignment method for calibration of hydrometers. Metrologia 41, pages S100–S104.

[78] S. Lorefice and A. Malengo. 2004. An image processing approach to calibration of hydrometers. Metrologia 41, pages L7–L10.

[79] J. Aguilera, J. D. Wright, and V. E. Bean. 2008. Hydrometer calibration by hydrostatic weighing with automated liquid surface positioning. Measurement Science and Technology 19. 015104.

[80] S. Lorefice and A. Malengo. 2006. Calibration of hydrometers. Measurement Science and Technology 17, pages 2560–2566.

[81] H. A. Bowman and Gallagher W. H. 1969. An improved high precision calibration procedure for reference standard hydrometers. Journal of Research of the National Bureau of Standards 73c, pages 57–65.

[82] S. V. Gupta and M. Nath. 1984. A method for calibrating low density hydrometer using a standard hydrometer calibrated for higher densities. OIML Bulletin 54, pages 7–10.

[83] M. G. Cox. 2002. The evaluation of key comparison data: An introduction. Metrologia 39, pages 587–588.

[84] M. G. Cox. 2002. The evaluation of key comparison data. Metrologia 39, pages 589–595.

[85] B. M. Wood and R. J. Douglas. 1998. Confidence-interval interpretation of a measurement pair for quantifying a comparison. Metrologia 35, pages 187–196.

[86] S. F. Hoerner. 1965. Fluid-dynamic drag. Published by the Author.

[87] J. N. Newman. 1980. Marine hydrodynamics. The Massachusetts Institute of Technology. ISBN 0-262-14026-8.

[88] E. Schmidt, W. Beckmann, and E. Pohlhausen. 1930. Das Temperatur- und Geschwindigkeitsfeld vor einer Wärme abgebenden senkrechten Platte bei natürlicher Konvektion. Forschung im Ingenieurwesen 1, pages 391–406.

[89] M. Gläser. 1990. Responce of apparent mass to thermal gradients. Metrologia 27, pages 95–100.

[90] M. Gläser and J.Y. Do. 1993. Effect of free convection on the apparent mass of 1 kg mass standards. Metrologia 30, pages 67–73.

[91] M. Gläser. 1999. Change of the apparent mass of weights arising from the temperatur differences. Metrologia 36, pages 183–197.

[92] C. Matilla, J. de Frutos, and N. Cereceda. 2004. Study of the free convection effect on a standard weight using an infrared thermography imaging system. Metrologia 41, pages 264–271.

[93] Y. S. Tian and T. G. Karayiannis. 2000. Low turbulence natural convection in an air filled square cavity. Part I: the thermal and fluid flow fields. International Journal of Heat and Mass Transfer 43, pages 849–866.

[94] S. Wakitani. 1998. Flow patterns of matural convection in an air-filled vertical cavity. Physics of Fluids 10, pages 1924–1928.

[95] J. Tang and H. H. Bau. 1998. Numerical investigation of the stabilization of the no-motion state of a fluid layer heated from below and cooled from above. Physics of Fluids 10, pages 1597–1610.

[96] G. Mana, C. Palmisano, A. Perosino, S. Pettorruso, A. Peuto, and G. Zosi. 2002. Convective forces in high precision mass measurements. Measurement Science and Technology 13, pages 13–20.

[97] T. Aberra, S. W. Armfield, M. Behnia, and G. D. McBain. 2006. Stability of natural convection boundary layer flow on an evenly heated vertical plate. In: AIP Conference Proceedings, volume 862, pages 456–460.

[98] Y. Zhou, R. Zhang, H. Staroselsky, and H. Chen. 2004. Numerical simulation of laminar and turbulent buoyancy-driven flows using a lattice Boltzmann based algorithm. International Journal of Heat and Mass Transfer 47, pages 4869–4879.

[99] L. Prandtl. 1904. Über Flüssigkeitsbewegung bei sehr kleiner Reibung. In: Proceedings of the Third International Mathematics Congress. Heidelberg.

[100] C. L. M. H. Navier. 1823. Mémoire sur les lois du mouvement des fluides. Memoires de l'Academie Royale des Sciences 6, pages 389–416.

[101] G. G. Stokes. 1845. On the theories of internal friction of fluids in motion. Transactions of the Cabbridge Philosophical Society 8, pages 287–305.

[102] F. P. Incropera and D. P. DeWitt. 1996. Fundamentals of heat and mass transfer. John Wiley and Sons. ISBN 0-471-30460-3.

[103] F. M. White. 1991. Viscous fluid flow. McGraw-Hill. ISBN 0-07-100995-7.

[104] H. Schlichting and K. Gersten. 2000. Boundary layer theory. Springer-Verlag. ISBN 3-540-66270-7.

[105] I. Pop and H. S. Takhar. 1993. Free convection from a curved surface. Zeitschrift für Angewandte Mathematik und Mechanik 73, pages 534–539.

[106] S. Ostrach. 1953. An analysis of laminar free convection flow and heat transfer about a flat plate parallel to the direction of the generating body force. Technical Report 1111, NACA.

[107] P. Giacomo. 1982. Equation for the determination of the density of moist air (1981). Metrologia 18, pages 33–40.

[108] R. S. Davis. 1992. Equation for the determination of the density of moist air (1981/1991). Metrologia 29, pages 67–70.

[109] A. Picard, R. S. Davis, M. Gläser, and K. Fujii. 2008. Revised formula for the density of moist air (CIPM-2007). Metrologia 45, pages 149–155.

[110] R. Mehta and P. Bradshaw. 1979. Design rules for small low speed wind tunnels. Aeronautical Journal 83, pages 443–449.

[111] S. Laine and J. Harjumäki. 1975. A theoretical study of axisummetric contractions for low-speed wind tunnels. Technical Report 75-A2, Helsinki university of technology.

[112] J. Bell and R. Mehta. 1989. Boundary-layer predictions for small low-speed contractions. AIAA Journal 27, pages 372–374.

[113] J. Gullman-Strand, O. Törnblom, B. Lindgran, G. Amberg, and A. Johansson. 2004. Numerical and experimental study of separated flow in a plane asymmetric diffuser. International Journal of Heat and Fluid Flow 25, pages 452–460.

[114] D. Sonntag. 1994. Advancements in the field of hygrometry. Meteorologische Zeitschrift 3, pages 51–66.

[115] L. P. Harrison. 1965. Measurement and control in science and industry, volume III, chapter Fundamental concepts and definitions relating to humidity, pages 3–70. Reinhold Publishing Corp.

[116] M. Heinonen. 1999. Intercomparison of the hydrometer calibration systems at the IMGC and the MIKES. Technical Report J9/1999, Centre for Metrology and Accreditation.

[117] H. Bettin and F. Spieweck. 1990. A revised formula for the calculation of alcoholometric tables. PTB-Mitteilungen 100, pages 457–460.

ISBN 978-952-5610-48-2
ISBN 978-952-5610-49-9 (PDF)
ISSN 1235-2704
ISSN 1797-9730 (PDF).

Sillanpää, Sampo

Thermodynamic studies in flow metrology

J3/2008

MIKES
Mittatekniikan keskus
Centre for metrology
and accreditation

• P.O.Box 9 (Tekniikantie 1) • 02151 ESPOO, FINLAND
• Tel. +358 10 6054 000 • Fax +358 10 6054 299
• www.mikes.fi